applied sciences

MDPI

Article

Determination of Natural Fundamental Period of Minarets by Using Artificial Neural Network and Assess the Impact of Different Materials on Their Seismic Vulnerability

Ercan Işık [1,*], Naida Ademović [2], Ehsan Harirchian [3,*], Fatih Avcil [1], Aydın Büyüksaraç [4], Marijana Hadzima-Nyarko [5,6], Mehmet Akif Bülbül [7], Mehmet Fatih Işık [8] and Barış Antep [9]

1 Department of Civil Engineering, Bitlis Eren University, Bitlis 13100, Turkey
2 University of Sarajevo—Faculty of Civil Engineering, 71000 Sarajevo, Bosnia and Herzegovina
3 Institute of Structural Mechanics (ISM), Bauhaus-Universität Weimar, 99423 Weimar, Germany
4 Çan Vocational School, Çanakkale 18 Mart University, Çanakkale 17400, Turkey
5 Department of Civil Engineering, Josip Juraj Strossmayer University of Osijek, VladimiraPreloga 3, 31000 Osijek, Croatia
6 Faculty of Civil Engineering, Transilvania University of Brașov, Turnului 5, 500152 Brașov, Romania
7 Department of Computer Engineering, Nevşehir Hacı Bektaş Veli University, Nevşehir 50300, Turkey
8 Department of Electrical-Electronics Engineering, Hitit University, Çorum 19030, Turkey
9 Independent Researcher, Bitlis 13100, Turkey
* Correspondence: eisik@beu.edu.tr (E.I.); ehsan.harirchian@uni-weimar.de (E.H.)

Abstract: Minarets are slender and tall structures that are built from different types of materials. Modern materials are also starting to be used in such structures with the recent developments in material technology. The seismic vulnerability and dynamic behavior of minarets can vary, depending on the material characteristics. Within this study's scope, thirteen different material types used in minarets in Türkiye were chosen as variables. A sample minaret model was chosen as an example with nine different heights to reveal how material characteristic change affects seismic and dynamic behavior. Information and mechanical characteristics were given for all the material types. Natural fundamental periods, displacements, and base shear forces were attained from structural analyses for each selected material. The empirical period formula for each material is proposed using the obtained periods, depending on the different minaret heights taken into consideration. At the same time, fundamental natural periods for the first ten modes and 13 different types of materials used in the study were estimated with the established Artificial Neural Network (ANN) model. The real periods from the experimental analyses were compared with the values estimated by the ANN using fewer parameters, and 99% of the results were successful. In addition, time history analyses were used to evaluate the seismic performance of the minaret (three different materials were considered). In this specific case, the acceleration record from the 2011 Van (Eastern Turkiye) earthquake (Mw = 7.2) was taken into consideration. Performance levels were determined for the minaret according to the results obtained for each material. It has been concluded that material characteristics significantly affect the dynamic and seismic behavior of the minarets.

Keywords: minaret; material; seismic behavior; dynamic analyses; ANN; period

check for updates

Citation: Işık, E.; Ademović, N.; Harirchian, E.; Avcil, F.; Büyüksaraç, A.; Hadzima-Nyarko, M.; Akif Bülbül, M.; Işık, M.F.; Antep, B. Determination of Natural Fundamental Period of Minarets by Using Artificial Neural Network and Assess the Impact of Different Materials on Their Seismic Vulnerability. *Appl. Sci.* **2023**, *13*, 809. https://doi.org/10.3390/app13020809

Academic Editors: Zhenhao Zhang, Yi Zhang, Sifeng Bi and Dixiong Yang

Received: 13 November 2022
Revised: 1 January 2023
Accepted: 3 January 2023
Published: 6 January 2023

Copyright: © 2023 by the authors. Licensee MDPI, Basel, Switzerland. This article is an open access article distributed under the terms and conditions of the Creative Commons Attribution (CC BY) license (https://creativecommons.org/licenses/by/4.0/).

1. Introduction

The combination of many building materials forms sections, and sections generate members, and members create structures. Humankind has built structures for different uses in their living spaces by using different materials to meet their needs for shelter, transportation, worship, and similar needs. With the developments in construction technologies and engineering, different building materials and construction techniques have also found a place in the construction sector [1–6]. Structures can be constructed in different types depending on functional requirements, choice of materials, technical knowledge, and

experience. Masonry structures are a widely preferred type of building, as they can be produced easily and at a low cost with the help of natural materials in the region where the building will be built. The history of masonry buildings dates back to the settled life of human beings. These structures are formed by placing elements made of adobe, clay, and/or natural stone on top of each other by applying binder material between them as carriers [7–13]. Natural stones were extensively used in every culture in the past and today for different purposes in structures. Especially in many masonry structures, natural stones are used together with a binding material [14,15]. The masonry construction was widely used and continues to be used in churches, mosques, minarets, synagogues, and temples that people built to meet their worship needs [16–20]. Minarets are an important part of mosques, where worship takes place in Islamic belief. The call to prayer is conducted from minarets, tall, thin, and fragile buildings that play a significant role in Islamic architecture. This research will use a minaret as an example. Due to the above-mentioned characteristics of the minarets, analysis of their behavior when subjected to horizontal loading is of particular significance. According to the advancements in building and construction technologies, minarets can now be built utilizing various building materials, including concrete, reinforced concrete (RC), and steel, in addition to the natural materials used in the regions where they are located. The mechanical properties of the materials used in minarets directly affect the behavior under loads, as in all engineering structures. In addition, by using different types of materials, the damage resistance, deformation capacity, and energy absorption capacity of engineering structures can be improved [21–24].

Even though some minarets have experienced numerous natural disasters, they have persevered through the years, much like many other historical monuments, to reach the present day. In particular, historical masonry minarets are considered within the scope of invaluable historical heritage in a symbolic sense and attract the attention of many different disciplines. Apart from examining the structural behavior of the minaret, the material properties (such as compressive and tensile strength, modulus of elasticity, unit volume weight, Poisson ratio, and porosity) were also determined using different techniques. Işık et al. [25] obtained the characteristics of the stone used in the five minarets, one of the landmarks of Bitlis, with non-destructive methods. They obtained the stresses that occur in all the minarets under the impact of earthquakes according to the updated seismic design code in Türkiye. Çalık et al. [26] used analytical and experimental techniques to examine the dynamic and static behavior of the Merkez Hacı Kasım Muhittin Mosque Minaret in Trabzon. Pekgökgöz et al. [27] identified the elastic modulus of the stone used to build the minarets of the Şanlıurfa Ulu Mosque by using ultrasonic test equipment. The investigation of the Carol I Mosque's minaret's response to seismic loads in Constanta, Romania, was conducted by Suliman et al. [28]. Işık and Antep [29] analyzed the seismic behavior of a historical masonry minaret in the Ahlat district, taking into account the previous seismic design code in Türkiye, and obtained the stress and displacement values. The impact of changing geometric characteristics on the earthquake behavior of different masonry historical minarets in Bursa was demonstrated by Livaoglu et al. [30]. The outcomes of vibration testing and numerical modeling in historical minarets by using various variables were compared by Oliveira et al. [31]. Nine medieval brick masonry minarets in Isfahan had structural evaluations conducted by Hejazi et al. [32] to account for dead loads, wind, temperature, and seismic effects. Ural and Çelik [33] investigated the dynamic behavior of seven masonry minarets in the city center of Aksaray (Türkiye). Carhoglu et al. [34] conducted a dynamic analysis using three earthquake acceleration records by considering the minarets of Hagia Sophia. The master's thesis of Güdü [35] examined wooden minarets with various construction systems and analyzed two of them in detail. Uğurlu and Karaşin [36] examined the four-legged minaret in Diyarbakır (Türkiye) using the finite element method (FEM) and analyzed the cracks formed in the minaret. The study of Kılıç et al. [37] concerns the seismic behavior of Hızırbey Mosque Minaret in the central district of Kırklareli (Türkiye). Seismic damage estimation of different ground motion levels in a historical brick masonry minaret was investigated using updated finite element models,

which were validated using the ambient vibration data [38]. Adam et al. [39] presented the condition assessment and structural analysis of the Al-Rifa'i minaret in Egypt. Khider and Al-Baghdadi [40] examined the seismic behavior of the Alkifil minaret in Iran. Each of these studies can be considered a case study.

These studies focused on FEM modeling, strengthening the masonry minarets, and identifying the minarets' structural characteristics and seismic behavior. Only the material properties currently used in the minaret were considered, and the variety of materials used in minarets was not examined in detail as in this study. Unlike many other studies, nine different minaret heights were considered in the structural analysis. In this study, unlike other studies, the effect of thirteen different building material types, which are widely used in today's minarets, on the earthquake behavior of minarets has been revealed. This study's main goal is to examine the behavior of minarets, which were built using different building materials and have an important place in Islamic architecture under the influence of earthquakes. This study aimed to reveal the impact of material mechanical properties on the seismic and dynamic behavior of minarets. Different building materials were taken into consideration, such as Ahlat stone, Bitlis stone, Küfeki stone, Diyarbakır basalt, brick, Andesite stone, natural stone, cut stone, adobe, Edremit travertine, Süphan basalt, Karamürsel Od stone, and the C25-concrete class. The mechanical properties of each material are taken directly from the literature, or if this information was unavailable, then the data were taken from the relevant standards. The sample minaret was modeled using the FEM, and structural analyses were performed for each material separately. Modal analysis of the minaret was conducted for each material type from which stresses and displacements were obtained. Eigenvalue analysis was used to determine the fundamental natural periods for different minaret materials and heights since the fundamental natural period of the building should be known for the analysis of a building under the influence of an earthquake. At the same time, natural fundamental periods for the first ten modes for 13 different types of materials used in the study were estimated with the established ANN model. The periods obtained from the structural analyses were compared with the values estimated by the ANN using fewer parameters, and 99% of successful results were obtained. In addition, linear time history analyses were implemented on the minaret (three different materials were considered) and performance levels were obtained. In this specific case, the 2011 Van earthquake acceleration records were utilized in the analyses. The empirical period formula has been proposed for each material, considering the minaret height used in this study. In addition, a comparison was made for seismic parameters utilizing the last two Turkish earthquake codes. It was checked whether each material's performance levels were achieved using top minaret displacements. The study will significantly contribute to other studies, including detailed structural analyses of many building materials. The novelty of this study is that structural analyses were carried out for thirteen different minaret materials and nine different minaret heights. With the help of the results obtained, specific empirical period formulas for each material have been proposed. In addition, the periods for these materials were determined by ANN. Both stresses and base shear forces and displacements were obtained for each material. The seismic performance of minarets made of different materials and heights was compared.

2. Information about Materials

Structures can be constructed using different types of materials. One important parameter that influences structures' behavior under loads is the structural material characteristics. These characteristics directly affect the behavior of structures under loads, especially seismic loads. In linear structural analysis, material features such as compressive and tensile strength, modulus of elasticity (E), unit volume weight, and Poisson's ratio (υ) are considered directly. These properties are very important for revealing the advantages and weaknesses of the materials and further for the development of the materials. In this study, a masonry minaret constructed with different types of materials was considered. Materials in masonry buildings may differ according to region. A total of thirteen different building

materials were taken into account for the sample minaret model within the scope of this study. The selected material properties were determined by using previous studies.

Ahlat stone is a product of Nemrut volcanism and is widely used in constructing houses, tombstones, gravestones, bridges, and minarets in the Lake Van basin. It continues to be widely used today as both a material for load-bearing walls and a covering material. These stones are available in various colors, such as light brown, dark brown (chestnut), and ash [41–44]. Ahlat stone is partially soft when removed from the ground and hardens under the influence of open air. The desired shapes can be easily acquired using the soft Ahlat stone by hand or machine [42,45].

Küfeki stone mostly contains limestone, fossiliferous limestone, and clayey limestone. Fossil limestone with $CaCO_3$ composition, known as "Küfeki stone" since the Ottoman Empire, is soft and easily shaped when first taken out of the quarry and stored afterward. Küfeki stone provides increased strength and long-term use benefits in terms of material and strength properties over time [46–48].

Diyarbakır Basalt has been used as a structural material for thousands of years because it is a local material and is abundant in the Diyarbakır region and is still widely used today. Diyarbakır-Karacadağ basalt deposits cover large areas in the Southeastern Anatolia Region of Türkiye. Basalt stone, formed due to the cooling of lava sprayed by Karacadağ, an ancient volcanic mountain, is among the hardest and most durable stones known in nature due to the metallic elements such as Fe, Si, Al, and Mg [49–52].

Bitlis stone is a product of Nemrut volcanism as Ahlat stone and is widely used in the Lake Van Basin region. It is a good thermal insulation material due to its hollow structure. Bitlis stone is partially soft when removed from the ground and hardens under the influence of open air. The desired shapes can be easily given to the soft Bitlis stone by hand or machine [53–55].

In the 19th century, depending on the technological developments experienced during the industrial revolution process, standard bricks were produced in Europe with increased physical qualities and mechanical strength [56]. Bricks (the main ingredient is clay) are classified as either fired or unbaked. Brick is widely used because of its cheapness, availability, and ease of use of soil material. In addition, it can be easily produced wherever there is suitable clay for brick production and is used as a building material in buildings [57–60].

Adobe is one of the oldest building materials obtained by mixing the soil with straw and water, pouring it into molds, and drying it first in the shade and then in the sun. The first stage in making adobe is where the clay is kneaded and prepared by hand. The second stage is the stage where it is shaped in molds and dried in the shade and then in the sun [57,61]. It is an indispensable material, especially for rural areas, it is a material of low cost, does not require the establishment of a production facility, and has a high thermal insulation value [62,63].

Andesite stone has been widely used in the construction industry in recent years, generally for the construction of pavements and wall coverings and as a load-bearing wall [64]. Andesite is a volcanic rock type found in different provinces in Türkiye. With their homogeneous structures, unfading colors, and unpolished, wiped, hammered, or rough-hewn surface forms, Andesites have been preferred in the domestic and foreign natural stone industry in recent years [65,66].

Travertine stones have an economic value due to their chemical composition and common use in the building industry [67]. In the study, Edremit (Van) travertine was taken into account. It is produced in quarries in the Edremit district of Van province, used as a building material in historical buildings, and used today as well [68].

Süphan basalt is a product of the Süphan volcanic mountain. Süphan volcano, formed in the Quaternary and has the character of a stratovolcano. It ejected its volcanic material in three stages. It produced dacite, breccia, and agglomerate in the first stage, basalt in the second stage, and dacite and trachyte in the last stage [69]. The volcanic material from the Süphan volcano continues to Van Lake in the south. Süte depression to the west of Mt. Süphan, Ahlat plain to the north of Mt. Nemrut, and Rahva plain between Bitlis massif

and Mt. Nemrut constitute the main plain areas of the province [69]. Süphan stone is used as a building material for different purposes in and around the region.

Karamürsel Od stone is a green volcanic tuff, known as Od stone, with quarries between Karamürsel-Gönceli near the coast. This stone, extracted from the quarries, was widely used by the Byzantines and the Ottomans due to its ease of processing. For example, Pertev Pasha Mosque was built in 1579 with Karamürsel stone and is placed in İzmit (Center). In addition, this stone was used in the Nuruosmaniye Mosque in Istanbul [70–72].

Another material considered within the scope of this study is natural stone. The natural stone properties used in the Trabzon Muhittin Mosque Minaret were determined by Çalık et al. [26], and these values were used in this study for natural stone. It is stated that the stone used in the minaret is a kind of andesite obtained from the Black Sea region [26].

Since most of the historic minarets in Türkiye were constructed using cut stone, this type of stone was also considered in this study. For the cut stone, the values obtained from the earthquake behavior and dynamic analyses of seven masonry minarets in Aksaray were taken into account by Ural and Çelik [33].

In addition to natural materials, concrete, used in today's minarets, was also considered in this study. For concrete, the C25 concrete grade was considered, and the properties of this concrete grade were taken directly from the Turkish Standard (TS500-2000) [73].

The modulus of elasticity, unit weight, and Poisson ratio values for all materials considered in this study are shown in Table 1.

Table 1. Characteristics of selected material types.

Material	Modulus of Elasticity (E) (MPa)	Unit Weight (t/m^3)	Poisson Ratio (υ)	References	Shear Modulus (G) (MPa)	Volumetric Modulus of Elasticity (K) (MPa)
Ahlat Stone	5000	2.45	0.20	[42,45]	2083	2778
C25 Concrete	30,000	2.50	0.20	[73]	12,500	16,667
Bitlis Stone	4006	2.30	0.22	[53–55]	1642	2385
Küfeki Stone	20,000	2.24	0.15	[46–48]	8696	9524
Diyarbakır Basalt	30,727	2.60	0.14	[49–52]	13,477	14,225
Brick	2985	2.10	0.25	[57,60]	1194	1990
Andesite Stone	12,240	2.20	0.30	[65,66]	4708	10,200
Natural Stone	8490	2.30	0.20	[26]	3538	4717
Cut Stone	4000	3.06	0.20	[33]	1667	2222
Adobe	880	2.04	0.20	[48,57]	367	489
Edremit Travertine	14,480	2.01	0.30	[67,68]	5569	12,067
Süphan Basalt	47,630	2.63	0.25	[65,69]	19,052	31,753
Karamürsel Od Stone	19,100	2.06	0.25	[70,72]	7640	12,733

In addition, for all materials, shear modulus (G) and volumetric modulus of elasticity (K) were obtained separately by using the Poisson's ratio (υ) and modulus of elasticity (E) obtained from the literature review, and all these values are given in Table 1.

The comparison of the elastic modulus (E) of the materials considered in the study is shown in Figure 1.

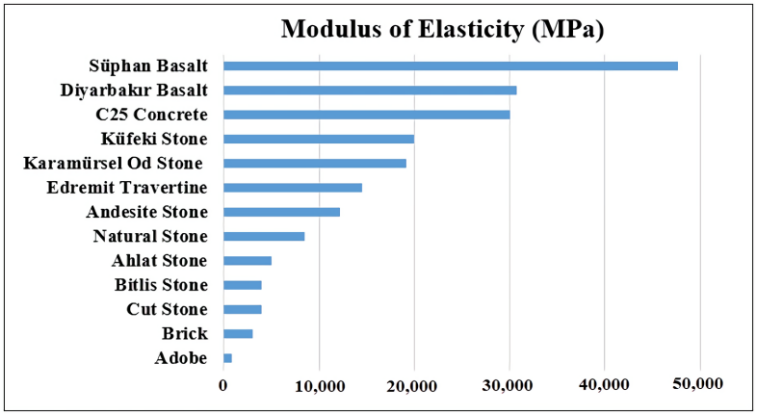

Figure 1. Comparison of the modulus of elasticity of the selected material types.

The modulus of elasticity measures the elastic deformation of the material under force. The modulus of elasticity indicates the stiffness of the material. The greater the modulus of elasticity, the material is more rigid, and the elastic strain is smaller. While the lowest periods were obtained for Süphan Basalt, which has the highest modulus of elasticity, the highest periods were obtained for adobe with the lowest modulus of elasticity.

3. Sample Minaret and Seismic Parameters for Structural Analysis

Minarets are tall and slender structures built by using different building materials, in which the azan is recited to indicate that the time of worship has come in mosques. They are tower-shaped structures that are typically placed either adjacent to the mosque or separated from the mosque. These structures are important not only from the religious point of view but as well from the architectural. In general, the minaret consists of a pulpit, transition section, body, balcony, the upper part of the body, end ornament, and spire. The parts of the sample minaret model are illustrated in Figure 2.

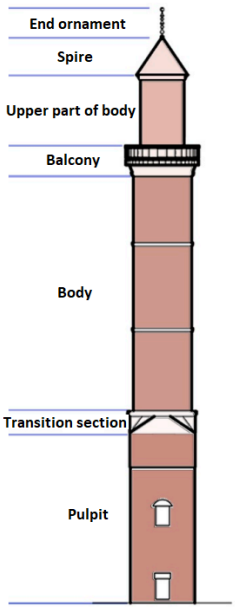

Figure 2. Parts of the minaret chosen as an example.

Türkiye Earthquake Hazard Maps (TEHM) and Türkiye Building Earthquake Code (TBEC-2018) [74] were considered while determining all the seismic parameters (peak ground acceleration (PGA), peak ground velocity (PGV), map spectral accelerations, and design spectral accelerations) needed for the structural analysis of the sample minaret.

Türkiye Earthquake Hazard Map (THEM), published in 2018, superseded the seismic risk map from 1996 by utilizing advancements in earthquakes and civil engineering, a current fault database, and earthquake catalogs [75,76]. Four different earthquake ground motion levels were specified with the current code and these levels are given in Table 2.

Table 2. Earthquake ground motion levels [74].

Earthquake Level	Return Period (Year)	Probability of Exceedance in 50 Years	Description
DD-1	2475	2%	Largest earthquake ground motion
DD-2	475	10%	Standard design earthquake ground motion
DD-3	72	50%	Frequent earthquake ground motion
DD-4	43	68%	Service earthquake ground motion

Türkiye Earthquake Hazard Map Interactive Web Earthquake Application (TEHMIWA) started to be used for obtaining the seismic parameters of any location. The geographic location of the Ulu Mosque was selected in Bitlis (Türkiye), and seismic parameters were obtained through TEHMIWA. In order to make comparisons, the local soil ground type ZB, given in TBEC-2018 [74], was considered the local soil class for all structural models. The properties of this soil class are given in Table 3.

Table 3. Properties of the local ground class type ZB [74].

Local Soil Class	Soil Type	Upper Average at 30 m		
		$(V_S)_{30}$ [m/s]	(N60) 30 [Pulse/30 cm]	(cu) 30 [kPa]
ZB	Less weathered, moderately strong rocks	760–1500	—-	—-

The PGV and PGA, which were obtained for the sample minaret's location for different probabilities of exceedance, are given in Table 4.

Table 4. Comparison of the PGA and PGV for different probabilities of exceedance.

Location	PGA (g)				PGV (cm/s)			
	Probabilities of Exceedance in 50 Year				Probabilities of Exceedance in 50 Year			
	2%	10%	50%	68%	2%	10%	50%	68%
Bitlis	0.490	0.260	0.106	0.077	28.215	15.081	6.508	4.847

The PGA and S_{DS} (design spectral acceleration coefficient) are also compared in Table 5 according to the two seismic design codes in Türkiye. The DD-2 earthquake ground motion level is selected as the standard earthquake motion level that is specified in the last two codes.

Table 5. Comparison of PGA and S_{DS} values over the last two seismic risk maps.

Location	TSDC-2007 Seismic Zone	TSDC-2007 PGA (g)	TBEC-2018 PGA (g)	PGA2007/PGA2018	$S_{DS\ 2007}$	$S_{DS\ 2018}$	$S_{DS\ 2007}/S_{DS\ 2018}$
Bitlis	1	0.400	0.260	1.54	1.000	0.553	1.81

The short period map spectral acceleration coefficient (S_S), the local ground coefficients (F_s and F_1), the map spectral acceleration coefficient for the 1.0 s period (S_1), the design spectral acceleration coefficient for the 1.0 s period (S_{D1}), the short period design spectral

acceleration coefficient (S_{DS}), the vertical elastic design spectrum corner periods (T_{AD}, T_{BD}), and the horizontal elastic design spectrum corner periods (T_A, T_B) were attained according to the different probabilities of exceedance by considering the specific geographical locations, which are shown in Table 6.

Table 6. Comparison of the seismic parameters for different earthquake ground motion levels.

Earthquake Level	S_S	S_1	F_S	F_1	S_{DS}	S_{D1}	T_A	T_B	T_{AD}	T_{BD}
DD-1	1.19	0.31	0.90	0.80	1.07	0.25	0.05	0.23	0.02	0.08
DD-2	0.61	0.17	0.90	0.80	0.55	0.14	0.05	0.25	0.02	0.08
DD-3	0.24	0.08	0.90	0.80	0.22	0.06	0.06	0.28	0.02	0.09
DD-4	0.18	0.06	0.90	0.80	0.16	0.04	0.06	0.28	0.02	0.09

The design spectra are created by fitting a smoothed envelope curve to the response spectra calculated from various ground motion acceleration records, taking into account the ground conditions and seismic characteristics of any region to account for the maximum earthquake effects that may occur [77–80]. The vertical and horizontal elastic design spectrum obtained through TEHMIWA for the selected location is shown in Figure 3.

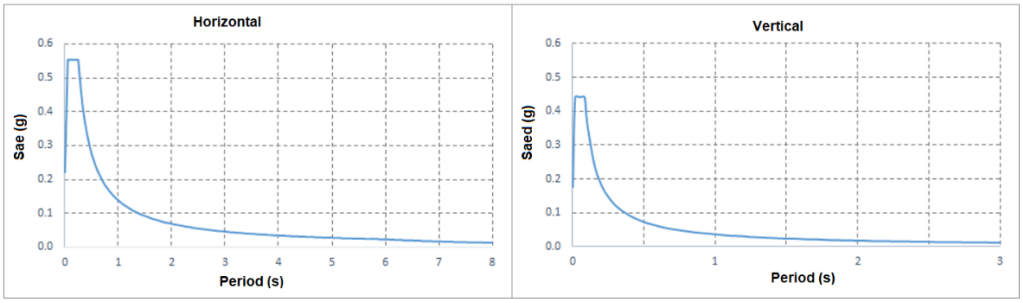

Figure 3. Horizontal/vertical elastic design spectrum used for the structural analysis.

4. Structural Analyses for Selected Materials

Older masonry structures' load-bearing systems differ from contemporary engineering ones. The behavior of masonry structures is very complex as it consists of elements made of various materials (units, joints, unit-joint interaction), creating a material of heterogeneous characteristics. Modeling masonry structures is a very complex task and a compromise between computational time and accuracy has to be made [81]. When assessing and creating masonry structures, modeling masonry walls is crucial. Numerical modeling with finite elements in masonry structures represents quite a long computational process [13,82]. Three modeling approaches, namely, a detailed micro-modeling approach, a simplified micro-modeling approach, and a macro-modeling approach, can be used to simulate masonry walls. Figure 4 illustrates these models.

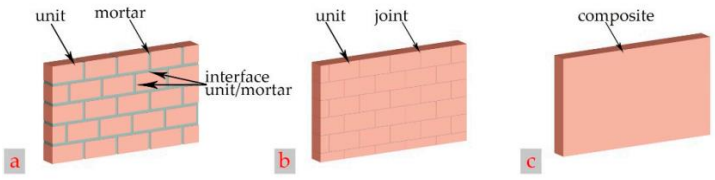

Figure 4. Modeling approaches for masonry structures: (**a**) detailed micro-modeling approach, (**b**) simplified micro-modeling approach, and (**c**) macro-modeling approach.

A FEM model of the reference minaret was generated using the macro modeling technique for this investigation. One of the most utilized methods in structural studies

of masonry constructions is the macro modeling methodology. This modeling must distinguish the binding material (mortar, etc.) utilized in the construction and the building elements. The masonry unit's and mortar's features were homogenized and recognized as composite masonry material in this modeling. Macro modeling is more convenient in practice as it requires less memory and time [7,83–86]. According to the assumptions set out by the software [83] utilized for the numerical modeling, the sign harmony and direction assumptions of the components employed in the finite element structural models are illustrated in Figure 5.

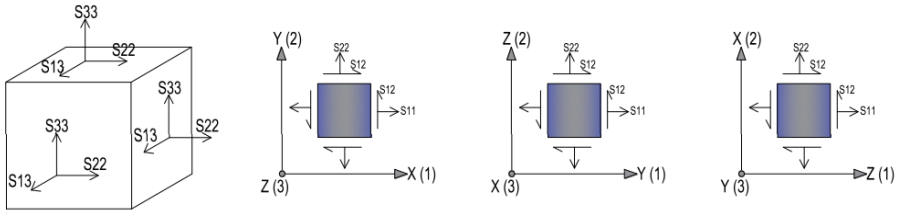

Figure 5. Sign alignment and direction assumptions.

As shown in Figure 5, S22 is vertical stress in the (Y) direction, S11 is vertical stress in the (X) direction, S33 is vertical stress in the (Z) direction, and (S12 = S21) are shear stresses in the X-Y plane.

Modeling and structural analyses for the sample minaret were performed using the ABAQUS software package. In this study, the minaret is considered separate from the mosque. The stairs were taken into account in the structural analyses and drawn together with the outer wall to avoid possible problems with the mesh. In order to make comparisons, the wall thicknesses were chosen at 40 cm for each material. Since height is one of the important factors affecting earthquake vulnerability in minarets, this value was chosen as a variable. Nine different minaret heights have been selected, such as 19.40 m, 21.40 m, 23.40 m, 25.40 m, 27.40 m, 29.40 m, 31.40 m, 33.40 m, and 35.40 m. In some figures and tables, the minaret model of 25.40 m in height has been considered an example. In the structural model, quadratic tetrahedral elements (C3D10) were chosen as the mesh type. The sample masonry minaret model consists of 17,673 elements and 33,325 nodes. Notably, 3D models of the sample minaret (H = 25.40 m) obtained from the software are shown in Figure 6.

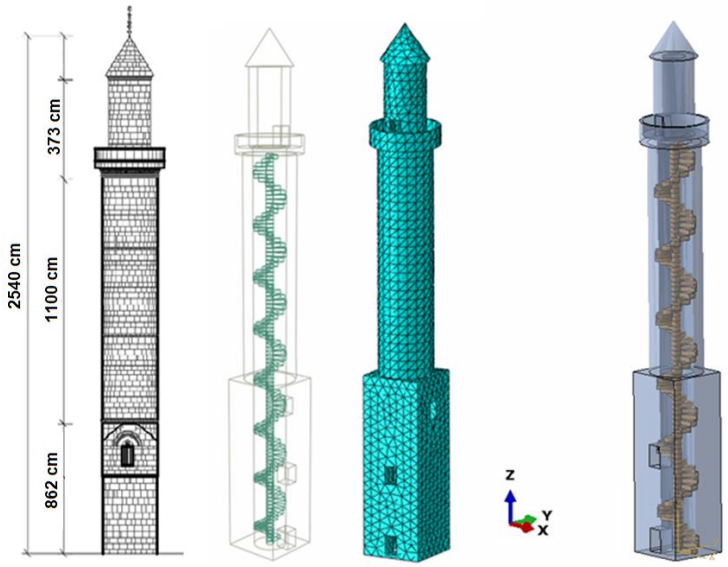

Figure 6. Sample minaret dimensions and 3D models (H = 25.40 m).

The modal analysis was performed in order to obtain the mode shapes, mass participation ratios, frequencies, and the free vibration periods of the structure. The dynamic features of the minaret were determined by the modal analyses. The first 5 mode shapes for the sample minaret for Bitlis Stone, whose total height is 25.40 m, are shown in Figure 7. Since the minaret has a square cross-section, similar shapes and values are obtained in the X and Y axes.

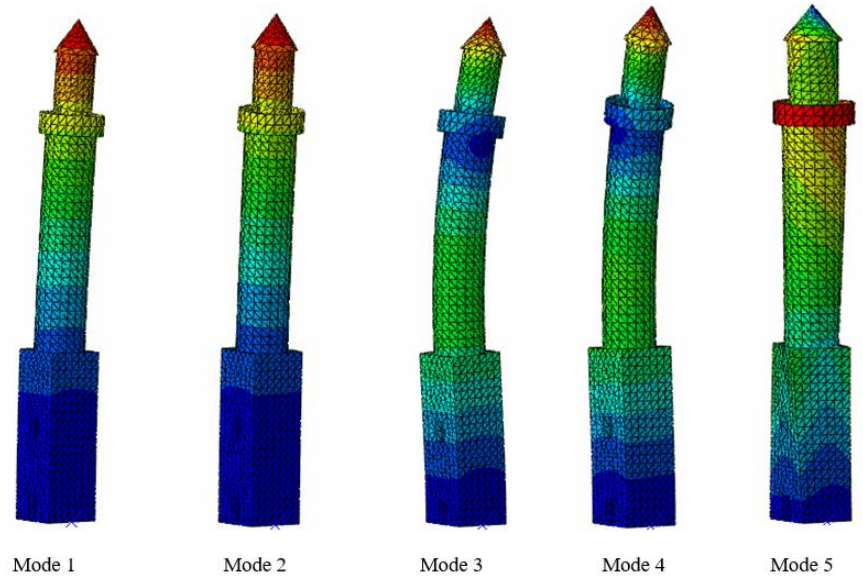

Figure 7. Mode shapes obtained for the sample minaret (H = 25.40 m).

4.1. Comparison of the Natural Fundamental Periods

The natural vibration period of the structure must be known for the analysis of any engineering structure under the earthquake's impact. The earthquake load on the structure is directly related to the structure's natural vibration period (or first mode period). The earthquake force that will affect the structure is a function of the period [87–91]. Natural vibration periods for different heights and material types were obtained according to the modal analysis. The comparison of fundamental natural periods is shown in Table 7. The first mode was taken into account for each height and material type while making the comparison. The mass participation ratios for the first ten modes in the X and Y directions were above 80% considering that the additional modes did not have much effect in the case of using different materials.

While the most rigid minaret was obtained when Süphan Basalt with the highest modulus of elasticity was used, the lowest stiffness value was obtained for adobe with the lowest modulus of elasticity. The comparison of the natural fundamental period obtained for the 1st mode for different materials for the sample minaret in the case of a minaret total height of 25.40 m is shown in Figure 8.

Table 7. The comparison of natural fundamental periods.

Height (m)	Periods (s)												
	Ahlat Stone	**C25 Concrete**	**Bitlis Stone**	**Küfeki Stone**	**Diyarbakır Basalt**	**Brick**	**Andesite**	**Natural Stone**	**Cut Stone**	**Adobe**	**Edremit Travertine**	**Süphan Basalt**	**Karamürsel Od Stone**
19.40	0.356	0.147	0.385	0.170	0.148	0.426	0.215	0.264	0.444	0.773	0.189	0.119	0.167
21.40	0.443	0.183	0.479	0.212	0.184	0.530	0.268	0.329	0.553	0.963	0.235	0.149	0.208
23.40	0.544	0.224	0.589	0.260	0.226	0.651	0.329	0.405	0.680	1.183	0.289	0.182	0.255
25.40	0.659	0.272	0.713	0.315	0.274	0.789	0.398	0.490	0.823	1.433	0.350	0.221	0.309
27.40	0.787	0.324	0.851	0.376	0.327	0.942	0.476	0.585	0.983	1.711	0.418	0.264	0.369
29.40	0.928	0.383	1.005	0.444	0.386	1.112	0.561	0.690	1.160	2.019	0.493	0.311	0.435
31.40	1.083	0.447	1.172	0.518	0.450	1.297	0.655	0.805	1.354	2.356	0.576	0.363	0.508
33.40	1.251	0.516	1.354	0.599	0.520	1.498	0.757	0.931	1.564	2.722	0.665	0.420	0.587
35.40	1.433	0.591	1.551	0.685	0.596	1.716	0.867	1.066	1.791	3.117	0.762	0.481	0.672

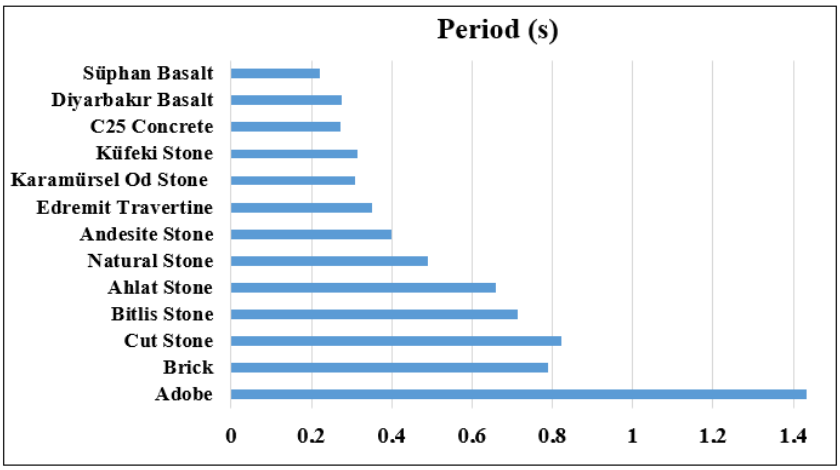

Figure 8. Comparison of the natural fundamental period of the 1st mode (H = 25.40 m).

4.2. Suggested Empirical Natural Fundamental Periods

Simple equations are often used to calculate the fundamental natural periods since it is only sometimes possible to make a detailed analysis of a building. Due to this issue, many researchers have proposed simplified equations. In these equations, the height of the building (H) is accepted as the basic parameter, and equations can be suggested with constants specific to the building material. For this purpose, many researchers have suggested the following relation depending on the material-dependent constants and the structure's height [92–97]:

$$T = cH^b \quad (1)$$

where H is the total height of the structures and c and b are constant. In this study, correlations have been developed for minarets made of different materials. In the equations, the first mode values were taken as references, and it was sufficient for the equation to provide the first mode period value in this study. In a time series analysis, a moving average is obtained only for a certain number of periodic averages, while the exponential moving average used in this study is a kind of moving average method that gives weight to the current frequency values. The empirical periods of natural stones defined in future studies can be obtained by using these relations. The relations between height and period obtained for different material types are given in Table 8.

In general, the formula ($T_1 = C_tH^{0.75}$) for the first period of the minarets is suggested. Here, $C_t = 0.05$, and H indicates the total minaret height. As can be seen from this formula, the material used in the minaret is not taken into account in the empirical period calculation. However, the recommended formulas for Ahlat stone, Bitlis stone, brick, and cut stone give the closest values to this empirical formula. While very high values are obtained for adobe, very low values are obtained for other remaining materials. Therefore, this study will be able to make important contributions in this respect.

The formulas were created by adding the trendline to allow the curves to be calculated for different heights. At this stage, the power trendline "which is the type of curve best used with datasets" that "compares measures that increase at a certain rate" is used. The exponential curve and the power trendline, which are typically used to represent measurements that rise at a given rate, are quite similar; however, the power trendline has a more symmetrical arc. A strength trendline cannot be created if the data contains zero or negative values. Obtaining the natural vibration period depending on the height of each material considered in the study has been presented in Figure 9.

Table 8. Recommended period relations for the material types.

Material Type	Suggested Empirical Relation
Ahlat Stone	$T = 0.0004H^{2.3234}$
C25 Concrete	$T = 0.0001H^{2.3222}$
Bitlis Stone	$T = 0.0004H^{2.3249}$
Küfeki Stone	$T = 0.0002H^{2.3253}$
Diyarbakır Basalt	$T = 0.0001H^{2.3245}$
Brick	$T = 0.0004H^{2.3252}$
Andesite	$T = 0.0002H^{2.3254}$
Natural Stone	$T = 0.0003H^{2.3271}$
Cut Stone	$T = 0.0004H^{2.3267}$
Adobe	$T = 0.0008H^{2.326}$
Edremit Travertine	$T = 0.0002H^{2.3268}$
Süphan Basalt	$T = 0.0001H^{2.3266}$
Karamürsel Od Stone	$T = 0.0002H^{2.3228}$

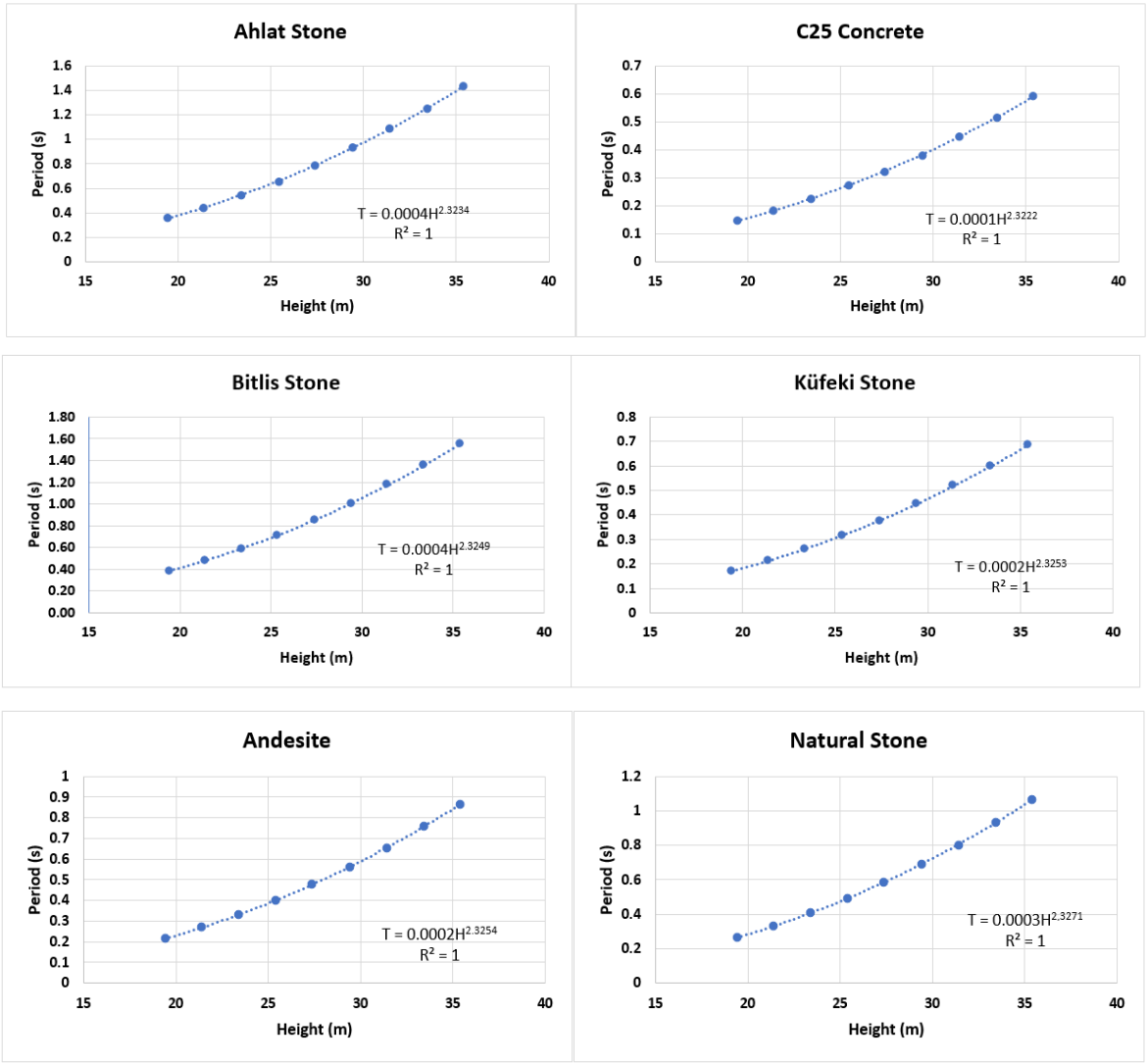

Figure 9. *Cont.*

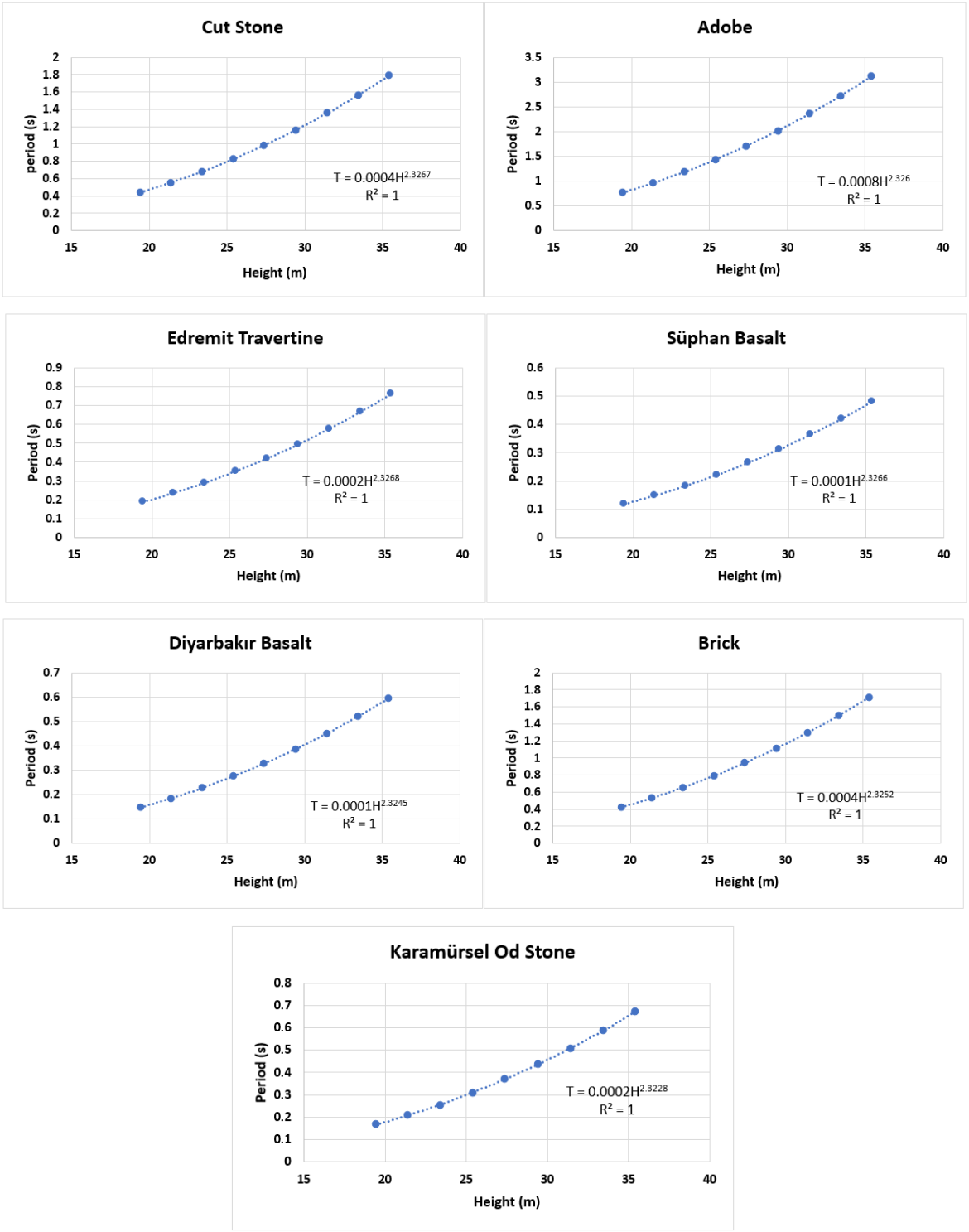

Figure 9. Obtaining the natural vibration period of the different materials considered in the study depending on the height.

4.3. Determination of Natural Fundamental Periods with ANN

Artificial Neural Networks (ANN) is a machine learning method frequently used in the literature [98,99]. ANN is based on the working principle of the biological neuron cell and consists of the connections established by many neuron cells with each other [100,101]. A basic ANN structure is given in Figure 10.

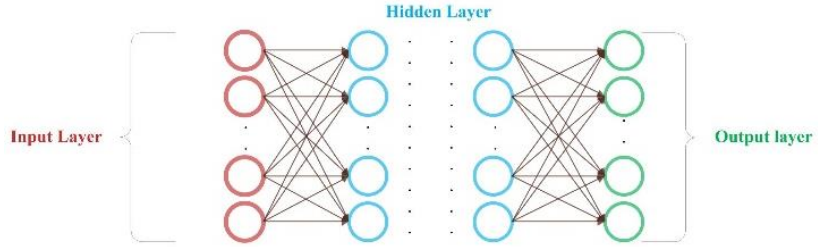

Figure 10. A sample ANN structure.

As shown in Figure 10, the ANN network consists of three layers. In the input layer, some inputs will start the information flow to the network. These inputs play an important role in accessing the predicted output information. The data entering the network from the input layer is transferred to the neuron cells in the next hidden layer. The information coming to each neuron cell is multiplied by the weights determined by the network and sent to the summation function. All information coming to the neuron cell is collected with this function, and the bias value determined by the network is added to it, creating a net input for the neuron cell [102]. Output information for the neuron cell is obtained by passing this net input through the activation function in the neuron cell. When the information passing through the hidden layers reaches the output layer, the output for the network is produced.

This part of the study aims to establish a feed-forward back propagation ANN network in calculating the fundamental natural periods for 13 different materials. In line with this goal, the input parameters to be used in the network were specified, as shown in Table 9.

Table 9. Input parameters.

Input Parameters	Description
Modulus of elasticity	The value given in the literature for each material has been taken into account.
Poisson ratio	The value given in the literature for each material has been taken into account.
H	It is the total height of the minaret, and 9 different heights are taken into account.
Mode	The top ten modes are considered for each material.
Material Type	13 different material types were considered.

With the input parameters presented in Table 9, natural period estimation of the network will be performed for different materials. The identification of different materials in the network within the input information was carried out, as shown in Table 10.

Table 10. Representation of different types of materials in the ANN network.

	Material Type												
	Bitlis Stone	**Andesite Stone**	**C25 Concrete**	**Diyarbakir Basalt**	**Natural Stone**	**Edremit Travertine**	**Karamursel Od Stone**	**Adobe**	**Cut Stone**	**Kufeki Stone**	**Suphan Basalt**	**Brick**	**Ahlat Stone**
ANN Values	1	2	3	4	5	6	7	8	9	10	11	12	13

In the study, 1400 fundamental natural periods were obtained from the different modulus of elasticity, the total height of the minaret, the Poisson ratio, and modes for 13 different types of materials. The data set created with these values will be used in the training (70%), validation (15%), and testing (15%) stages of the ANN. In this study, MATLAB programming language was preferred because of its flexible structure and easy coding of multidimensional problems [103]. While establishing the network structure, some parameters affect the performance of the network and need to be determined. These parameters are the algorithm to be used in the training of the network, the learning function, the activation functions that provide the translation of the information, the

number of hidden layers, and the number of neurons in these layers. Many learning algorithms, learning functions, and activation functions in network structures can be built with MATLAB programming language. In line with the experimental studies, trainlm (Levenberg-Marquardt) is used as the training function, and learngdm (Gradient Descent Momentum) is used as the adaptation learning function in the created network structure, while logsig (Log-Sigmoid) in the hidden layer and the tansig (Hyperbolic Tangent Sigmoid) activation function in the output layer are preferred. There is one hidden layer in the established network structure and ten neuron cells in this hidden layer. The ANN structure used in the natural fundamental period estimations is shown in Figure 11.

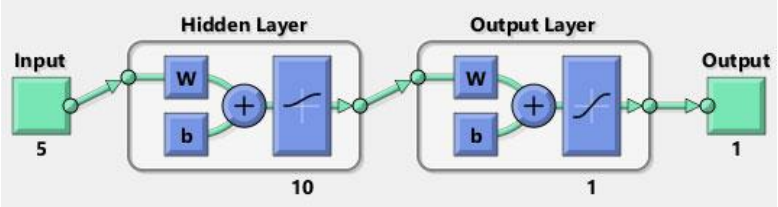

Figure 11. ANN model for natural fundamental period estimation.

The network structure presented in Figure 10 was first trained with the obtained data set. The performance of the network in the training process is shown in Figure 12.

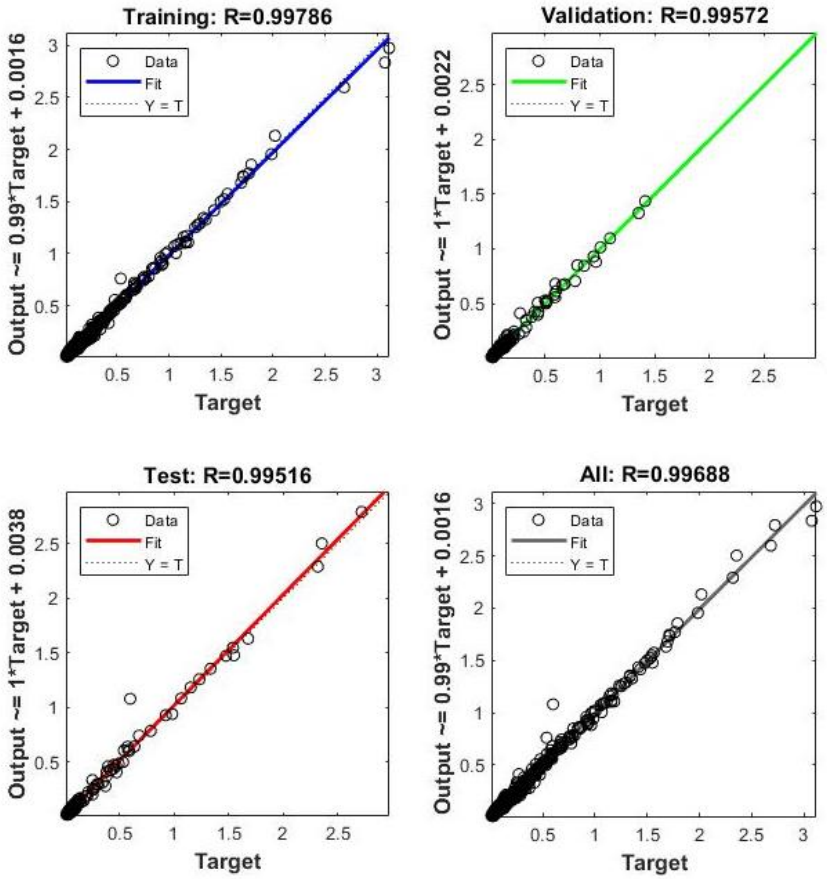

Figure 12. Regression graphs of the established ANN model.

According to the regression graphs presented in Figure 12, it can be seen that the established network structure's target line in training, validation, and test overlaps with the fit line and that the data is concentrated on these lines. It shows that the network has a high estimation rate in the training process. Successful results were obtained as a result

of experimental analyses with the obtained ANN structure, and the fundamental natural periods presented in Table 6, which the network had yet to see before, were estimated. In the experimental studies, it has been observed that the target line and the fit line are separated from each other in the ANN structures established with different network parameters, and the R values decrease as the estimation data moves away from these lines. This shows that the network structures established with different parameters exhibit low performance. The fundamental natural periods obtained by ANN for 13 different types of materials are shown in Table 11.

Table 11. ANN results in natural fundamental period estimation.

Mode	Periods (s)												
	Bitlis Stone	Andesite Stone	C25 Concrete	Diyarbakır Basalt	Natural Stone	Edremit Travertine	Karamürsel Od Stone	Adobe	Cut Stone	Küfeki Stone	Süphan Basalt	Brick	Ahlat Stone
1	0.725	0.417	0.288	0.265	0.502	0.339	0.292	1.395	0.790	0.317	0.212	0.780	0.651
2	0.707	0.399	0.252	0.262	0.547	0.334	0.311	1.345	0.850	0.298	0.207	0.778	0.620
3	0.165	0.088	0.065	0.063	0.115	0.068	0.063	0.285	0.178	0.065	0.050	0.174	0.148
4	0.134	0.079	0.056	0.058	0.107	0.066	0.064	0.240	0.162	0.053	0.057	0.151	0.115
5	0.112	0.062	0.048	0.049	0.091	0.054	0.054	0.194	0.138	0.043	0.051	0.128	0.095
6	0.087	0.042	0.037	0.039	0.073	0.040	0.042	0.154	0.112	0.032	0.039	0.101	0.074
7	0.068	0.027	0.029	0.031	0.059	0.030	0.033	0.125	0.091	0.025	0.030	0.081	0.058
8	0.054	0.018	0.024	0.025	0.048	0.023	0.026	0.103	0.075	0.020	0.023	0.065	0.046
9	0.043	0.013	0.020	0.021	0.039	0.018	0.022	0.085	0.062	0.017	0.019	0.052	0.037
10	0.035	0.011	0.017	0.018	0.032	0.015	0.018	0.070	0.050	0.015	0.016	0.042	0.030

When the estimated values found and the periods obtained as a result of modal analysis (Table 7) are compared, the absolute error values of the created ANN structure for each mode and each type of material are shown in Table 12.

Table 12. Absolute error values of ANN for each mode and material type.

Mode	Periods (s)												
	Bitlis Stone	Andesite Stone	C25 Concrete	Diyarbakır Basalt	Natural Stone	Edremit Travertine	Karamürsel Od Stone	Adobe	Cut Stone	Küfeki Stone	Süphan Basalt	Brick	Ahlat Stone
1	0.008	0.016	0.012	0.002	0.009	0.008	0.018	0.012	0.033	0.038	0.011	0.009	0.017
2	0.026	0.015	0.008	0.011	0.006	0.005	0.009	0.067	0.043	0.059	0.009	0.010	0.008
3	0.003	0.003	0.001	0.007	0.000	0.008	0.003	0.003	0.011	0.044	0.013	0.001	0.008
4	0.036	0.006	0.029	0.018	0.005	0.029	0.012	0.005	0.026	0.087	0.014	0.007	0.007
5	0.012	0.014	0.021	0.004	0.015	0.026	0.010	0.029	0.034	0.014	0.008	0.022	0.014
6	0.004	0.008	0.012	0.001	0.010	0.018	0.000	0.022	0.025	0.004	0.003	0.016	0.009
7	0.011	0.001	0.006	0.007	0.002	0.001	0.015	0.008	0.006	0.023	0.006	0.007	0.001
8	0.012	0.000	0.008	0.007	0.001	0.004	0.017	0.005	0.004	0.021	0.007	0.004	0.001
9	0.004	0.003	0.001	0.002	0.004	0.003	0.012	0.009	0.011	0.003	0.004	0.005	0.002
10	0.011	0.001	0.009	0.004	0.002	0.007	0.014	0.002	0.000	0.018	0.007	0.002	0.001

As a result of the findings, the mean square error (MSE) value of the structure established with ANN was calculated as 0.0003, and the root means square error (RMSE) value was 0.0175. In light of this information, successful results were obtained with ANN in the natural fundamental period estimation. These results show that the proposed ANN network structure successfully estimates the natural basis period. In addition, the proposed ANN network structure and the network parameters that should be used in solving such a problem have also been determined. With the obtained architecture, the natural basis period estimation can be determined quickly and accurately.

4.4. Comparison of Stress, Base Shear, and Displacements for Minaret (H = 25.40 m)

Structural analyses of the sample minaret for different types of material were performed considering DD-2 earthquake ground motion level which is the standard earthquake ground motion level with a 10% probability of exceedance in 50 years (recurrence period of 475 years). Three different building materials were taken into account such as adobe, Süphan basalt, and C25 concrete, and examples for the stress diagrams are presented in the following Figures (Figures 13–15). The stress diagrams in the minaret made

of Süphan basalt with the highest modulus of elasticity (E = 47,630 MPa) are shown in Figure 13.

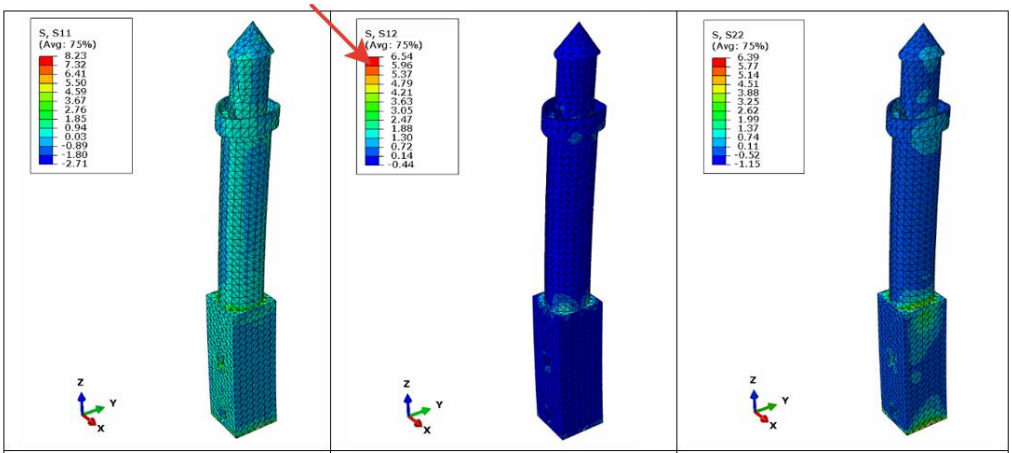

Figure 13. Stress diagrams for Süphan Basalt (H = 25.40 m).

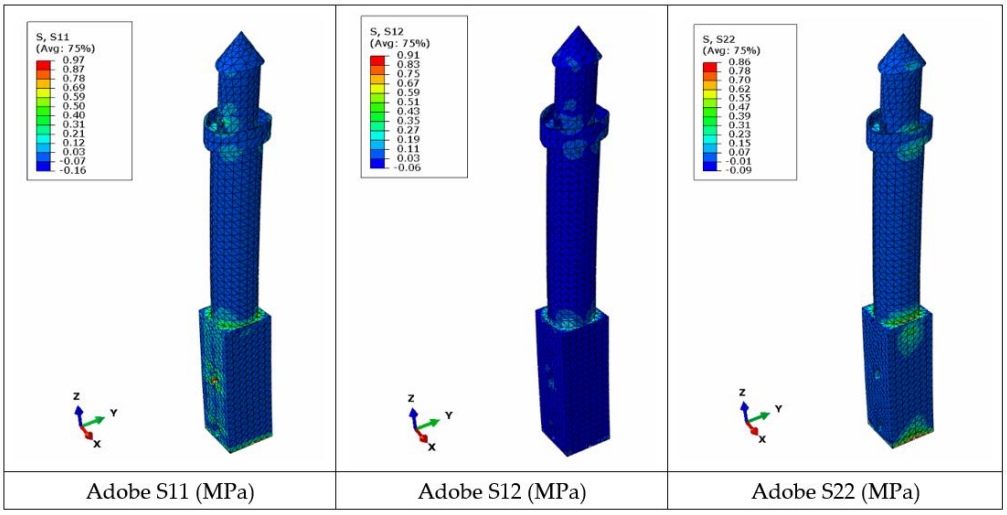

Figure 14. Stress diagrams for adobe (H = 25.40 m).

The stress diagrams in the minaret made of adobe material with the lowest modulus of elasticity (E = 880 MPa) are shown in Figure 14.

The stress diagrams in the minaret made of C25 concrete, having a modulus of elasticity of E = 30,000 MPa, which is significantly different from other materials considered in this study, are shown in Figure 15.

The comparison of the obtained results for all material types is shown in Table 13.

The material with a higher modulus will have the least period and maximum stiffness and attract more shear than the material with the least modulus. In this context, the highest displacements and base shear were obtained for adobe with the smallest modulus of elasticity, while the lowest displacements and base shear were obtained for Süphan Basalt with the highest modulus of elasticity. On the other hand, the situation is the opposite of the resulting stresses.

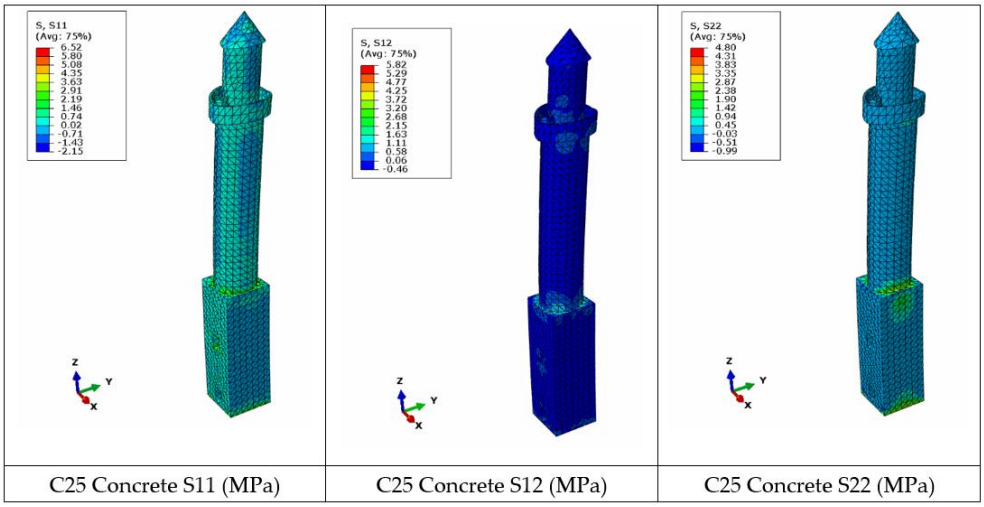

Figure 15. Stress diagrams for C25 concrete (H = 25.40 m).

Table 13. Comparison of the analysis results for different material types (H = 25.40 m).

Material	Displacement (mm)	Base Shear Force (N)	S11 (MPa)	S12 (MPa)	S22 (MPa)
Ahlat stone	175.5	1.89×10^6	2.66	2.35	2.00
C25 concrete	71.8	2.98×10^6	6.52	5.82	4.80
Bitlis stone	190.2	1.74×10^6	2.42	2.04	1.88
Küfeki stone	83.4	2.42×10^6	4.67	4.52	2.51
Diyarbakır basalt	72.4	3.08×10^6	6.20	6.04	3.28
Brick	210.1	1.55×10^6	1.81	1.68	1.92
Andesite stone	105.4	2.07×10^6	5.06	3.50	4.58
Natural stone	129.9	1.97×10^6	3.34	2.97	2.48
Cut stone	219.8	2.23×10^6	2.03	2.35	1.98
Adobe	384.8	1.14×10^6	0.97	0.91	0.86
Edremit travertine	92.6	2.03×10^6	5.26	3.64	4.71
Süphan basalt	50.9	3.29×10^6	8.23	6.54	6.39
Karamürsel Od stone	81.8	2.25×10^6	5.31	4.21	4.13

4.5. Performance Levels of Minaret (H = 25.40 m)

In this study, the performance levels of different materials were determined by using the roof drifts of the minaret model. For this, the limit value assumptions specified in the Türkiye Earthquake Risk Management Guide for Historic Buildings (TERMFHB-2017) [104] were taken into account, and these limit states are given in Figure 16. It is remarked that it is adequate to conduct linear calculation for the Damage Limitation (DL) performance level and one of the linear or non-linear calculation methods for the Controlled Damage (CD) and Prevention of Collapse (PC) performance levels. In the case of DL, the drift ratio under earthquake does not exceed the 0.3% limit. In the case of CD, the drift ratio under earthquake does not exceed the 0.7% limit and in the case of PC, the drift ratio under earthquake does not exceed the 1% limit.

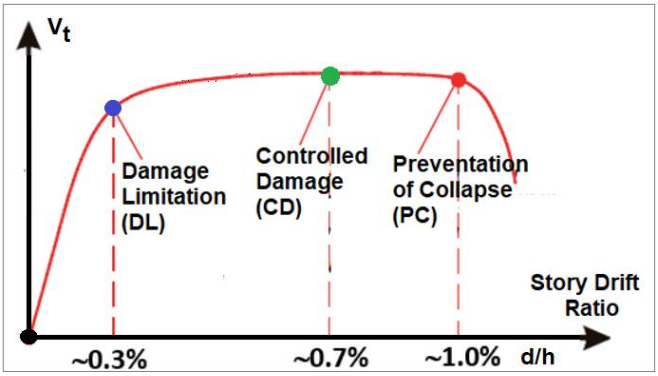

Figure 16. Pushover curve and limit states [104].

A response spectrum analysis was performed using the Abaqus finite element model. This analysis can be used to calculate the peak response (stress, displacement, etc.) of the minaret to a particular base motion. Linear analyses were performed on the minaret's models. In structures with sufficient ductility, the horizontal part of the curve is prominent and long. However, in cases where ductile behavior is limited, as in masonry structures in general, the Controlled Damage (CD) and Prevention of Collapse (PC) performance levels are in close proximity. In the fully brittle behavior, the structure reaches power exhaustion without inelastic deformation. In this type of brittle behavior, evaluation according to deformation is insignificant, so a small earthquake load reduction coefficient is accepted, and the structure is evaluated according to strength.

The performance levels obtained for the DD-2 earthquake predicted in TBEC-2018 and specified as the design earthquake ground motion level are given in Table 14.

Table 14. Design earthquake displacement controls (H = 25.40 m).

Material Type	Roof Displacement (mm)	Peak Drift Ratio (%)	DL < 0.3%		CD < 0.7%		PC < 1%	
Adobe	384.8	1.51	76.2	×	178	×	254	×
Brick	210.1	0.83	76.2	×	178	×	254	√
Cut stone	219.8	0.87	76.2	×	178	×	254	√
Bitlis stone	190.2	0.75	76.2	×	178	×	254	√
Ahlat stone	175.5	0.69	76.2	×	178	√	254	√
Natural stone	129.9	0.51	76.2	×	178	√	254	√
Andesite stone	105.4	0.41	76.2	×	178	√	254	√
Edremit travertine	92.6	0.36	76.2	×	178	√	254	√
Karamürsel Od stone	81.8	0.32	76.2	×	178	√	254	√
Küfeki stone	83.4	0.33	76.2	×	178	√	254	√
C25 concrete	71.8	0.28	76.2	√	178	√	254	√
Diyarbakır basalt	72.4	0.29	76.2	√	178	√	254	√
Süphan basalt	50.9	0.20	76.2	√	178	√	254	√

Here, the × sign indicates that the performances are not insufficient, and the √ sign indicates that the performances are sufficient. All materials except adobe were found to be sufficient for the prevention collapse performance level for the standard earthquake ground motion level. Cut stone, brick, Bitlis stone, and adobe materials did not provide the recommended performance level for controlled damage. All other materials provided this level of performance. While C25 concrete, Diyarbakır, and Süphan basalt had a sufficient performance for the damage limitation, other materials were not sufficient at this performance level.

4.6. Time-History Analyses for Different Materials

In this study, time-history analyses were also performed for the sample minaret made of three different materials such as adobe, Süphan basalt, and C25 concrete. The numerical analysis of the equation of motion, which is constructed by taking into account the mass, stiffness, and damping parameters of the structure, under a chosen acceleration record, is called a time-history analysis. In this method, the earthquake load reduction coefficient is also used in the calculation of the stress and internal forces in the sections to consider the inelastic behavior of the structure. Time-history analyses were performed by using the acceleration records of the 2011 Van earthquake, which happened close to the selected location for the reference minaret. The Van earthquake acceleration-time curve for South-North was used in this analysis and is shown in Figure 17.

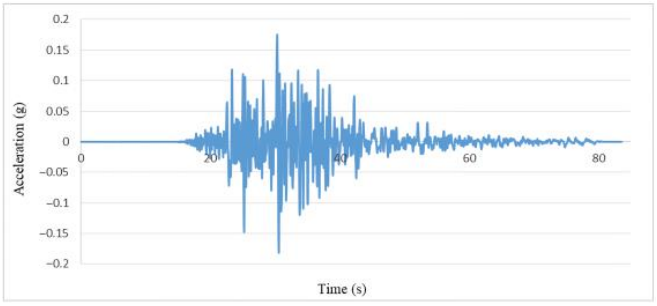

Figure 17. South-North acceleration-time curve of the 2011 Van earthquake.

The time-displacement curves of the sample minaret for the 2011 Van earthquake were given in Figures 18–20 for adobe, Süphan Basalt, and C25 concrete, respectively.

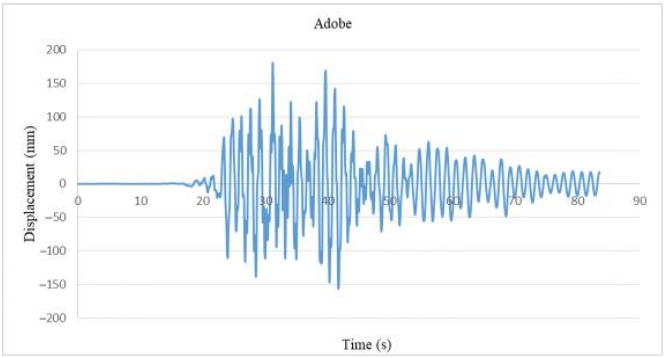

Figure 18. Time-displacement curve for minaret made of adobe.

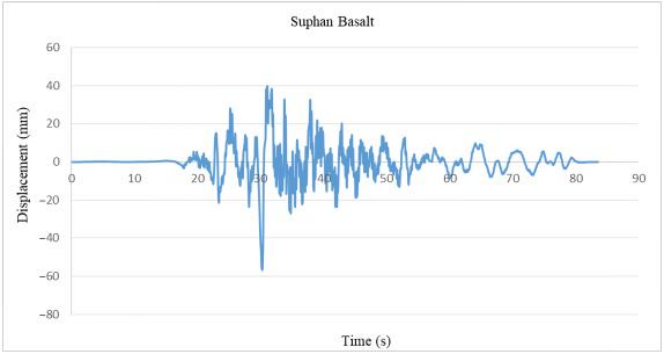

Figure 19. Time-displacement curve for minaret made of Süphan basalt.

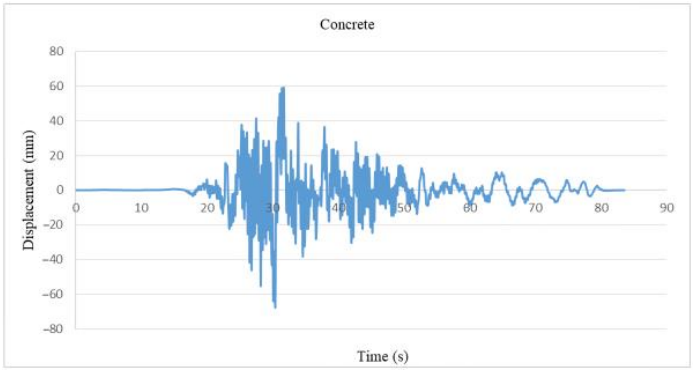

Figure 20. Time-displacement curve for minaret made of C25 concrete.

The comparison of performance levels for the minaret made of three different materials is given in Table 15.

Table 15. Comparison of performance levels of three different material types (H = 25.40 m).

Material Type	Natural Fundamental Period (s)	Roof Displacement (mm)	Roof Drift Ratio (%)	DL < 0.3%		CD < 0.7%		PC < 1%	
Adobe	1.433	180.27	0.71	76.2	×	178	×	254	√
C25 concrete	0.272	67.29	0.26	76.2	√	178	√	254	√
Süphan basalt	0.221	56.6	0.22	76.2	√	178	√	254	√

While the × sign indicates that the performances are not insufficient, the √ sign indicates that they are sufficient performances. C25 concrete, Süphan basalt, and adobe were found to be sufficient for the prevention collapse performance level for the standard earthquake ground motion level. Adobe material did not provide the recommended performance level for controlled damage and damage limitation. Both other materials provide these performance levels.

5. Results and Conclusions

Although the history of masonry buildings dates back to ancient times, they could have been and could still be built from different building materials. Within the scope of this study, the usage of different material types for a sample minaret model was examined in detail. Within the scope of the study, previous studies for thirteen different types of minaret materials were compiled, and material properties were determined. In addition to the naturally obtained materials, the concrete material widely used today has also been considered. Structural analyses were performed for each material type, respectively.

The modulus of elasticity, which measures the elastic deformation of materials under force, has the highest value for Süphan basalt and the lowest value for adobe. Among the materials considered, the material with the highest unit volume weight value is cut stone, while the material with the lowest value is Edremit travertine. While Poisson's ratio has the highest value for Diyarbakır basalt, the lowest value is obtained for Edremit travertine.

In this study, the predicted values in the last two earthquake hazard maps and the seismic design codes used in Türkiye were compared for the selected location because of the need to use site-specific design spectra for the minaret according to the current seismic design code. As a result, the predicted PGA on the updated seismic hazard map (2018) for the selected location was lower than the previous one (2007). This may be different for different locations.

It is known that the change of the design spectra obtained specifically for the site will significantly change the target displacement values predicted for the building performance.

Therefore, in cases where the target displacement values need to be adequately represented, it is impossible to determine the performance levels of structures under the earthquake effect accurately.

While the highest period was obtained for adobe with the lowest modulus of elasticity, the lowest period was obtained for Süphan basalt with the highest modulus of elasticity. This situation remained valid for frequency values as well. As the elasticity modulus increases in the material, the period values decrease, causing the structure to behave more rigidly. The material elasticity modulus is a parameter that directly affects the rigidity of the structures. The period values obtained from the structural analysis results for all different materials.

Meanwhile, empirical period formulas based on height were proposed for each material. Minaret wall thickness was chosen equally for all materials used in the sample model. It will be useful to examine the thickness variation in future studies. The proposed empirical period correlations were obtained only according to the height considered. This study will contribute to developing the relations obtained by considering different heights for these materials.

According to the structural analyses considering the response spectrum, the highest roof draft was obtained at 38.5 cm for the adobe with the lowest modulus of elasticity. The lowest roof draft was obtained for Süphan basalt at 5.1 cm. The highest base shear force was obtained for Süphan basalt, while the lowest base shear force was obtained for adobe. The tensile, compressive, and shear stresses have the highest values for Süphan basalt, and the lowest values have been obtained for adobe.

Due to the random location of the minaret considered in Bitlis, the analysis was carried out in the time history by selecting the acceleration records of the 2011 Van (Eastern Türkiye) earthquake, which is the closest and most effective earthquake to this region. The time-history analyses were performed for minarets made of three different materials. This analysis was also carried out for concrete which can be classified in the non-natural material class, and adobe and Süphan basalt, which have the lowest and highest modulus of elasticity, respectively. A displacement of 18 cm was obtained for the adobe, where the displacement of Süphan basalt was 5.7 cm. With the increase of the modulus of elasticity, more rigid structures are obtained, and as a result, they have a smaller displacement under the effect of earthquakes.

According to the analysis results, the maximum shear force and stresses that occur in the structure are high because the total weight of the material with a higher unit volume weight is also high. In addition, the maximum displacement in the structure increases with the weight of the structure. Therefore, a material with a high modulus of elasticity has a higher maximum shear force and stress levels. In contrast, the maximum displacement and period are lower in the materials with a lower modulus of elasticity. It is understood from the analysis results that the change in the Poisson ratio in the materials does not make a significant change in the displacement, basic shear force, and period values and that the stresses (S11, S12, and S22) increase when the Poisson ratio increases.

While minarets made from C25 concrete, Diyarbakır, and Süphan basalt are within limits for the DL drift ratio for the design earthquake, all other materials do not meet this limit condition. CD status was not met for minarets made of adobe, brick, cut stone, and Bitlis stone but was satisfied for minarets made of other materials. It was not met for minarets made of all materials in the case before the collapse. While all DL conditions were met for the minarets made of C25 concrete and Süphan basalt, the minaret made of adobe fulfilled only the PC damage limit state. At the same time, successful results were obtained with fewer parameters in the natural fundamental period estimation thanks to a generated feed-forward and backpropagation ANN structure. The findings also determined the proper network structure and the necessary adjustments and parameters. These parameters constitute a pioneering model for decision support systems in natural fundamental period calculations.

There is a significant consistency among all the results obtained. In this context, it is important that the structural analyses required for the material selection and design to be used in the minaret-type structures, which are delicate due to their construction style, are carried out with precision. While the ductility of such slender and tall structures should be as high as possible, it has been observed that even if the stresses that will occur in the structure can be carried, in case of constructed with masonry technique with low ductility, damage caused by brittle fractures in big earthquakes cannot be avoided.

In market investigations between Süphan basalt, adobe, and concrete materials, adobe was obtained as the most economical material, while the material with the highest cost was Süphan basalt. While the cost of concrete was three times the cost of adobe, Süphan basalt was obtained at seven times the cost of adobe.

The scope of this paper was minarets with a single balcony and a circular cross-section. Future investigations can be conducted for minarets with two or three balconies and different cross sections. This study was also carried out by taking into account equal minaret thickness in order to make comparisons. In the codes, only the minaret height, or the minaret height and the base width, are taken into account without paying attention to the material differentiation in the empirical relations related to the masonry buildings. This study proposes new empirical formulas for determining the natural periods of minarets constructed of different materials. These proposed formulas will be a source for experimental studies to be carried out on minarets using these materials. This study will also be a source for the structural analysis of minarets.

Author Contributions: Conceptualization, M.A.B., E.I., F.A., E.H., N.A., M.H.-N., A.B., B.A. and M.F.I.; methodology, E.I., F.A., A.B., M.A.B. and M.F.I.; software F.A., M.A.B., B.A., N.A. and M.H.-N.; validation, N.A., E.H., A.B., M.F.I. and E.I.; formal analysis, N.A., M.H.-N. and E.H.; investigation, E.I., F.A., A.B., B.A., M.A.B. and M.F.I.; resources, N.A., E.H. and M.H.-N.; data curation, E.I., A.B., F.A. and M.A.B.; writing—original draft preparation, E.I., E.H., N.A., M.A.B., A.B. and B.A.; writing—review and editing, E.I., N.A. and M.H.-N.; visualization, N.A., M.F.I. and E.H.; supervision, E.I., M.A.B., F.A. and A.B.; project administration, E.I.; funding acquisition, E.H. All authors have read and agreed to the published version of the manuscript.

Funding: This research received no external funding.

Institutional Review Board Statement: Not applicable.

Informed Consent Statement: Not applicable.

Data Availability Statement: Data sharing is not applicable.

Conflicts of Interest: The authors declare no conflict of interest.

References

1. Bilgin, H. Typological classification of churches constructed during post-Byzantine period in Albania. *Gazi Uni. J. Sci. Part B Art Humanit. Des. Plan.* **2015**, *3*, 1–15.
2. Hadzima-Nyarko, M.; Ademovic, N.; Pavic, G.; Sipos, T.K. Strengthening techniques for masonry structures of cultural heritage according to recent Croatian provisions. *Earthq. Struct.* **2018**, *15*, 473–485.
3. Karasin, I.B.; Isik, E. Protection of Ten-Eyed Bridge in Diyarbakır. *Bud. Archit.* **2016**, *15*, 87–94. [CrossRef]
4. Hendry, A.W.; Sinha, B.P.; Davies, S.R. *Design of Masonry Structures*; CRC Press: Boca Raton, FL, USA, 2017.
5. Işık, E.; Antep, B.; Büyüksaraç, A. Structural analysis and mapping of historical tombs in Ahlat District (Bitlis, Turkey). *JCR E GFOS* **2019**, *10*, 22–35. [CrossRef]
6. Lourenço, P.B.; Milani, G.; Tralli, A.; Zucchini, A. Analysis of masonry structures: Review of and recent trends in homogenization techniques. *Can. J. Civ. Eng.* **2007**, *34*, 1443–1457. [CrossRef]
7. Lourenço, P.B. Computations on historic masonry structures. *Prog. Struct. Eng. Mater.* **2002**, *4*, 301–319. [CrossRef]
8. D'Altri, A.M.; Sarhosis, V.; Milani, G.; Rots, J.; Cattari, S.; Lagomarsino, S.; Sacco, E.; Tralli, A.; Castellazzi, G.; de Miranda, S. Modeling strategies for the computational analysis of unreinforced masonry structures: Review and classification. *Arch. Comput. Methods Eng.* **2020**, *27*, 1153–1185.
9. Bilgin, H.; Ramadani, F. Numerical study to assess the structural behavior of the Bajrakli Mosque (Western Kosovo). *Adv. Civ. Eng.* **2021**, *2021*, 4620916. [CrossRef]

10. Biçen, V.S.; Işık, E.; Arkan, E.; Ulu, A.E. A study on determination of regional earthquake risk distribution of masonry structures. *ArtGRID J. Arch. Eng. Fine Arts* **2020**, *2*, 74–86.
11. Lourenço, P.B.; Rots, J.G. Multisurface interface model for analysis of masonry Structures. *J. Eng. Mech.* **1997**, *123*, 660–668. [CrossRef]
12. Işık, E.; Harirchian, E.; Bilgin, H.; Jadhav, K. The effect of material strength and discontinuity in RC structures according to different site-specific design spectra. *Res. Eng. Struct. Mater.* **2021**, *7*, 413–430. [CrossRef]
13. Giordano, A.; Mele, E.; Luca, A. Modelling of historical masonry structures. Comparison of different approaches through a case study. *Eng. Struct.* **2002**, *24*, 1057–1069. [CrossRef]
14. Figueiredo, C.; Folha, R.; Maurício, A.; Alves, C.; Aires-Barros, L. Contribution to the technological characterization of two widely used Portuguese dimension stones: The "Semi-rijo" and "MocaCreme" stones. In *Natural Stone Resources for Historical Monuments*; Prĭkryl, R., Tőrők, A., Eds.; Geological Society Special Publications: London, UK, 2010; Volume 333, pp. 153–164.
15. Pereira, D.; Marker, B. The Value of Original Natural Stone in the Context of Architectural Heritage. *Geosciences* **2016**, *6*, 13. [CrossRef]
16. Cescatti, E.; Salzano, P.; Casapulla, C.; Ceroni, F.; Da Porto, F.; Prota, A. Damages to masonry churches after 2016–2017 Central Italy seismic sequence and definition of fragility curves. *Bull. Earthq. Eng.* **2020**, *18*, 297–329. [CrossRef]
17. Ashayeri, I.; Biglari, M.; Formisano, A.; D'Amato, M. Ambient vibration testing and empirical relation for natural period of historical mosques; case study of eight mosques in Kermanshah, Iran. *Constr. Build. Mater.* **2021**, *289*, 123191. [CrossRef]
18. Erdil, B.; Tapan, M.; Akkaya, İ.; Korkut, F. Effects of structural parameters on seismic behaviour of historical masonry minaret. *Period. Polytech. Civ. Eng.* **2018**, *62*, 148–161. [CrossRef]
19. Işık, M.F.; Işık, E.; Harirchian, E. Application of IOS/Android rapid evaluation of post-earthquake damages in masonry buildings. *Gazi Mühendislik Bilim. Derg.* **2021**, *7*, 36–50.
20. Fan, Y.; Song, S.; Huang, J.; Lu, Y.; Liu, J.; Zhen, Q.; Bashir, S. Study on weathering mechanism of masonry bricks of ancient temples in Shanxi province using DingxiangHongfu temple masonry brick. *Constr. Build. Mater.* **2019**, *222*, 500–510. [CrossRef]
21. Tariq, H.; Jampole, E.A.; Bandelt, M.J. Fiber-hinge modeling of engineered cementitious composite flexural members under large deformations. *Eng. Struct.* **2019**, *182*, 62–78. [CrossRef]
22. Tariq, H.; Jampole, E.A.; Bandelt, M.J. Development and application of spring hinge models to simulate reinforced. *J. Struct. Eng.* **2021**, *147*, 04020322. [CrossRef]
23. Bandelt, M.J.; Frank, T.E.; Lepech, M.D.; Billington, S.L. Bond behavior and interface modeling of reinforced high-performance fiber-reinforced cementitious composites. *Cem. Concr. Compos.* **2017**, *83*, 188–201. [CrossRef]
24. Aksoylu, C.; Özkılıç, Y.O.; Hadzima-Nyarko, M.; Işık, E.; Arslan, M.H. Investigation on improvement in shear performance of reinforced-concrete beams produced with recycled steel wires from waste tires. *Sustainability* **2022**, *14*, 13360. [CrossRef]
25. Işık, E.; Harirchian, E.; Arkan, E.; Avcil, F.; Günay, M. Structural analysis of Five Historical Minarets in Bitlis (Turkey). *Buildings* **2022**, *12*, 159. [CrossRef]
26. Çalık, İ.; Demirtaş, B.; Bayraktar, A.; Türker, T. Analytical and experimental methods used in investigating the structural safety of pile stone minarets: The example of the minaret of muhittin mosque in Trabzon. *VakıflarDerg* **2012**, *38*, 121–139.
27. Pekgökgöz, R.K.; İzol, G.; Avcil, F.; Gürel, M.A. Determination of the elastic modulus of the building stone of Sanliurfa Grand Mosque minaret by of using ultrasonic testing machine. *Harran Üniversitesi Mühendislik Derg.* **2018**, *3*, 35–45.
28. Suliman, S.; Gramescu, A.M.; Gelmambet, S. Modelling the structure of Carol I Mosque Minaret taken into account the seismic evaluation. *IOP Conf. Ser. Mater. Sci. Eng.* **2021**, *1138*, 012040. [CrossRef]
29. Işık, E.; Antep, B. Structural analysis of historical masonry minaret in Ahlat. *BEU. J. Sci.* **2018**, *7*, 46–56.
30. Livaoğlu, R.; Baştürk, M.H.; Doğangün, A.; Serhatoğlu, C. Effect of geometric properties on dynamic behavior of historic masonry minaret. *KSCE J. Civ. Eng.* **2016**, *20*, 2392–2402. [CrossRef]
31. Oliveira, C.S.; Çaktı, E.; Stengel, D.; Branco, M. Minaret behavior under earthquake loading: The case of historical Istanbul. *Earthq. Eng. Struct. Dyn.* **2012**, *41*, 19–39. [CrossRef]
32. Hejazi, M.; Moayedian, S.M.; Daei, M. Structural analysis of Persian historical brick masonry Minarets. *J. Perform. Constr. Facil.* **2016**, *30*, 04015009. [CrossRef]
33. Ural, A.; Celik, T. Dynamic analyses and seismic behavior of masonry minarets with single Balcony. *Aksaray Uni. J. Sci. Eng.* **2018**, *2*, 13–27. [CrossRef]
34. Çarhoğlu, A.I.; Usta, P.; Korkmaz, K.A. Seismic behavior investigation of historical minaret structures: Hagia Sophia case. *Uluslararası Teknol. Bilim. Derg.* **2013**, *5*, 36–43.
35. Güdü, D. The Structural System of Timber Minarets and their Earthquake Behaviors. Ph.D. Thesis, Bursa Uludag University, Bursa, Turkey, 2021.
36. Uğurlu, M.A.; Karaşin, A. Evaluation of the structural damages of the Four-Legged Minaret. In Proceedings of the 12th International Congress on Advances in Civil Engineering, Istanbul, Turkey, 21–23 September 2016.
37. Kılıç, İ.; Bozdoğan, K.B.; Aydın, S.; Gök, S.G.; Gündoğan, S. Determination of dynamic behaviour of tower type structures: The case of KırklareliHızırbey Mosque minaret. *J. Polytech.* **2020**, *23*, 19–26.
38. Nohutcu, H. Seismic failure pattern prediction in a historical masonry minaret under different earthquakes. *Adv. Civil Eng.* **2019**, *2019*, 8752465. [CrossRef]

39. Adam, M.A.; El-Salakawy, T.S.; Salama, M.A.; Mohamed, A.A. Assessment of structural condition of a historic masonry minaret in Egypt. *Case Stud. Constr. Mater.* **2020**, *13*, e00409. [CrossRef]
40. Khider, T.A.; Al-Baghdadi, H.A. Dynamic response of historical masonry minaret under seismic Excitation. *Civ. Eng. J.* **2020**, *6*, 142–155. [CrossRef]
41. Işik, E.; Aydin, M.C.; Ülker, M. Performance evaluation of a historical tomb and seismicity of the region. *Bitlis Eren Uni. J. Sci. Technol.* **2016**, *6*, 59–65.
42. Şimşek, O.; Erdal, M. Investigation of some mechanical and physical properties of the Ahlat stone (Ignimbrite). *Gazi Uni. J. Sci.* **2004**, *17*, 71–78.
43. Avşar, E.; Işık, E. Environmental toxicity characteristics of Nemrut volcanism pyroclastic, Bitlis/Turkey case. *Sigma J.Eng. Natural Sci.* **2020**, *38*, 1203–1215.
44. Isik, E.; Antep, B.; Buyuksarac, A.; Isik, M.F. Observation of behavior of the Ahlat Gravestones (TURKEY) at seismic risk and their recognition by QR code. *Struct. Eng. Mech.* **2019**, *72*, 643–652.
45. Erdal, M.; Şimşek, O. Investigation of usability of Ahlat Stone (ignimbrite) waste as stone powder in concrete. *Politek. Derg.* **2011**, *14*, 173–177.
46. Erözmen, T.; Ündül, Ö.; Aysal, N. Evaluation of different cleaning techniques applied on Küfeki Stones used for historical buildings in İstanbul. *Pamukkale Üniversitesi Mühendislik Bilim. Derg.* **2020**, *26*, 1413–1418.
47. Kumral, M.; Şans, G.; Yalçın, C.; Kaya, M.; Budakoğlu, M. The effects of physical and chemical properties on the formation of historical kufeki stone in Çatalca (Istanbul). *Niğde Ömer Halisdemir Üniversitesi Mühendislik Bilim. Derg.* **2019**, *8*, 278–287.
48. Demirkan, D.S. Effects of the Mortar Thickness to Masonry Buildings, Masonry Buildings, Historical Buildings, Anisotrop Materials, Anisotropic Solutions. Ph.D. Thesis, Fen Bilimleri Enstitüsü, İstanbul Teknik Üniversitesi, İstanbul, Türkiye, 2014.
49. Yıldız, S.; Işık, N.; Keleştemur, O. Investigation of the mechanical properties of basalt stones in the Diyarbakır-Karacadağ. *Sci. Eng. J. Fırat Univ.* **2008**, *20*, 617–626.
50. Karasin, A.; Hadzima-Nyarko, M.; Işık, E.; Doğruyol, M.; Karasin, I.B.; Czarnecki, S. The effect of basalt aggregates and mineral admixtures on the mechanical properties of concrete exposed to sulphate attacks. *Materials* **2022**, *15*, 1581. [CrossRef] [PubMed]
51. Aslan, D.; Sariişik, A. Comparison of characteristic properties of basalts, limestone and stream materials used in bituminous hot mix in Diyarbakir Region. *Harran Üniversitesi Mühendislik Derg.* **2019**, *3*, 243–250.
52. Kahveci, A.E.; Kadayifçi, A. Investigation structural properties of basalt stone in Diyarbakir Region. *Uluslararası Teknol. Bilim. Derg.* **2013**, *5*, 56–69.
53. Işık, E.; Büyüksaraç, A.; Avşar, E.; Kuluöztürk, M.F.; Günay, M. Characteristics and properties of Bitlis ignimbrites and their environmental implications. *Mater. Construcción* **2020**, *70*, 214. [CrossRef]
54. Koralay, T.; Özkul, M.; Kumsar, H.; Çelik, S.B.; Pektaş, K. The importance of mineralogical, petrographic and geotechnical studies in historical heritage: The Bitlis Castle case (Bitlis-Eastern Anatolia). *Selcuk. Univ. J. Engineer. Sci. Technol.* **2014**, *2*, 54–68. [CrossRef]
55. Koralay, T.; Özkul, M.; Kumsar, H.; Celik, S.B.; Pektaş, K. The effect of welding degree on geotechnical properties of an ignimbrite flow unit: The Bitlis castle case (Eastern Turkey). *Environ. Earth Sci.* **2011**, *64*, 869–881. [CrossRef]
56. Çiftçi, A.; Yergün, U. Osmanlı mimarlığının modernleşme sürecinde temel bir yapı malzemesi: Tuğla. *Şehir Düşünce Merk.* **2012**, 177–191.
57. Eroğlu, M.; Akyol, A.A. Brick and tile as antique building material: Boğsak Island Byzantium Settlement sampling. *Sanat Tasarım Derg.* **2017**, *20*, 141–162. [CrossRef]
58. Şişman, C.B.; Kocaman, İ.; Gezer, E. A study on physical and mechanical properties of bricks produced and commonly used in agricultural buildings around Tekirdag. *Tekirdağ Ziraat Fakültesi Derg.* **2016**, *3*, 32–40.
59. Nohutcu, H.; Demir, A.; Ercan, E.; Hokelekli, E.; Altintas, G. Investigation of a historic masonry structure by numerical and operational modal analyses. *Struct. Des. Tall Spéc. Build.* **2015**, *24*, 821–834. [CrossRef]
60. Korkmaz, A.; Çarhoğlu, A.I.; Orhon, A.V.; Nuhoğlu, A. Farklı yapısal malzeme özelliklerinin yığma yapı davranışına etkisi. *Nevşehir Bilim Teknol. Derg.* **2014**, *3*, 69–78. [CrossRef]
61. Abhilash, H.N.; Hamard, E.; Beckett, C.T.S.; Morel, J.C.; Varum, H.; Silveira, D.; Ioannou, I.; Illampas, R. Mechanical behaviour of earth building materials. In *Testing and Characterisation of Earth-Based Building Materials and Elements*; Springer: Cham, Switzerland, 2022; pp. 127–180.
62. Austin, G.S. Adobe as a building material. *New Mex. Geol.* **1984**, *6*, 69–71.
63. Özgünler, S.A.; Gürdal, E. From past to present earth based building material: Adobe. *Restorasyon Konserv. Çalışmaları Derg.* **2012**, *9*, 29–37.
64. Şimşek, O. Investigation of engineering properties of the pink andesite stones of Çankırı-Korgun region. *Gazi Üniversitesi Fen Bilim. Derg.* **2003**, *16*, 619–625.
65. Sariisik, A.; Sariisik, G.; Şentürk, A. Applications of glaze and decor on dimensioned andesites used in construction sector. *Constr. Build. Mater.* **2011**, *25*, 3694–3702. [CrossRef]
66. Ceylan, H. Freeze-thaw cycles Isparta andesite stone effect of the physicomechanical properties. *Tek. Bilim. Derg.* **2016**, *6*, 7–12.
67. Erdoğan, O.; Özvan, A. Evaluation of strength parameters and quality assessment of different lithotype levels of Edremit (Van) Travertine (Eastern Turkey). *J. Afr. Earth Sci.* **2015**, *106*, 108–117. [CrossRef]

68. Karabaşoğlu, A.K.; Karaoğlu, Ö.; Kuvanç, R. Van Çevresindeki (Doğu Türkiye) Urartu yerleşim merkezlerinde (van kalesi, aşağı ve yukarı anzaf, çavuştepe, ayanis, toprakkale, zivistan, keçikıran, aliler, körzüt ve menua kanalı tarihi yerleri) kullanılan kayaçlara ilişkin petrografik gözlemler. *Türkiye Jeol. Bülteni* **2021**, *64*, 199–222.
69. Elmastaş, N. Geothermal spring in Bitlis Province. *Doğu Coğrafya Derg.* **2008**, *13*, 89–104.
70. Kahraman, N.; Arıkan, R. Başbakanlık Osmanlı arşivi belgelerinde Karamürsel taşı ve İzmit bölgesi diğer taşocakları. In *Uluslararası Kara Mürsel Alp Kocaeli Tar. Sempozyumu II Kocaeli Türkiye*; Ottoman Archives: Istanbul, Turkey, 2016; Volume 3, pp. 1863–1876.
71. Özgünler, S.A. A Research about the Conservation of Volcanic Tuffs Used in Historic Buildings: As a Case of "Od Tasi" (Dasitic Volcanic Tuff). Ph.D. Thesis, Fen Bilimleri Enstitüsü, İstanbul Teknik Üniversitesi, İstanbul, Türkiye, 2007.
72. Angı, S. Natural stones used in the antique buildings and monuments on historical peninsula of Istanbul their characteristics and state of conservation. *Restorasyon Konserv. Çalışmaları Derg.* **2010**, *6*, 31–42.
73. *TS500*; Requirements for Design and Construction of Reinforced Concrete Structures. Türkiye Standards Institution: Ankara, Turkey, 2000.
74. *TBEC-2018*; Turkish Building Earthquake Code. T.C. ResmiGazete: Ankara, Türkiye, 2018.
75. Işık, E. A comparative study on the structural performance of an RC building based on updated seismic design codes: Case of Turkey. *Challenge* **2021**, *7*, 123–134. [CrossRef]
76. Işık, E. Comparative investigation of seismic and structural parameters of earthquakes (M $\geq$ 6) after 1900 in Turkey. *Arab. J. Geosci.* **2022**, *15*, 971. [CrossRef]
77. Kale, Ö.; Akkar, S. An auxiliary tool to build ground-motion logic-tree framework for probabilistic seismic hazard assessment, *3.* . In Proceedings of the Türkiye Deprem Mühendisliği ve Sismoloji Konferansı, İzmir, Türkiye, 14–16 October 2015.
78. Işık, E.; Harirchian, E. A comparative probabilistic seismic hazard analysis for Eastern Turkey (Bitlis) based on updated hazard map and its effect on regular RC structures. *Buildings* **2022**, *12*, 1573. [CrossRef]
79. Işık, E.; Avcil, F.; Harirchian, E.; Arkan, E.; Bilgin, H.; Özmen, H.B. Architectural characteristics and seismic vulnerability assessment of a historical masonry minaret under different seismic risks and probabilities of exceedance. *Buildings* **2022**, *12*, 1200. [CrossRef]
80. Kutanis, M.; Ulutaş, H.; Işik, E. PSHA of Van province for performance assessment using spectrally matched strong ground motion records. *J. Earth Syst. Sci.* **2018**, *127*, 99. [CrossRef]
81. Ademovic, N.; Hrasnica, M.; Oliveira, D.V. Pushover analysis and failure pattern of a typical masonry residential building in Bosnia and Herzegovina. *Eng. Struct.* **2013**, *50*, 13–29. [CrossRef]
82. Akan, A.E.; Başok, G.; Er, A.; Örmecioğlu, H.T.; Koçak, S.Z.; Cosgun, T.; Uzdil, O.; Sayin, B. Seismic evaluation of a renovated wooden hypostyle structure: A case study on a mosque designed with the combination of Asian and Byzantine styles in the Seljuk era (14th century AD). *J. Build. Eng.* **2021**, *43*, 103112. [CrossRef]
83. Abaqus, G. *Abaqus 6.11*; Dassault Systemes Simulia Corporation: Providence, RI, USA, 2011.
84. Pande, G.N.; Liang, J.X.; Middleton, J. Equivalent elastic modul for unit masonry. *Comput. Geotech.* **1989**, *8*, 243–265. [CrossRef]
85. Laurenco, P.B.; Rots, J.G.; Blaauwendraad, J. Two approaches for the analysis of masonry structures: Micro and macro-modeling. *Heron* **1995**, *40*, 1995.
86. Ademović, N.; Hadzima-Nyarko, M.; Zagora, N. Seismic vulnerability assessment of masonry buildings in Banja Luka and Sarajevo (Bosnia and Herzegovina) using the macroseismic model. *Bull. Earthq. Eng.* **2020**, *18*, 3897–3933. [CrossRef]
87. Aksoylu, C.; Arslan, M.H. Investigation of periods of frame type reinforced concrete buildings according to different empirical approach. *Bitlis Eren Üniversitesi Fen Bilim. Derg.* **2019**, *8*, 569–581. [CrossRef]
88. Bilgin, H.; Hadzima-Nyarko, M.; Isik, E.; Ozmen, H.B.; Harirchian, E. A comparative study on the seismic provisions of different codes for RC buildings. *Struct. Eng. Mech.* **2022**, *83*, 195–206.
89. Aksoylu, C.; Mobark, A.; Arslan, M.H.; Erkan, İ.H. A comparative study on ASCE 7-16, TBEC-2018 and TEC-2007 for reinforced concrete buildings. *Rev. Construcción.* **2020**, *19*, 282–305. [CrossRef]
90. Nikoo, M.; Hadzima-Nyarko, M.; Khademi, F.; Mohasseb, S. Estimation of fundamental period of reinforced concrete shear wall buildings using self organization feature map. *Struct. Eng. Mech.* **2017**, *63*, 237–249.
91. Jamadin, A.; Ibrahim, Z.; Jumaat, M.Z.; Hosen, M.A. Serviceability assessment of fatigued reinforced concrete structures using a dynamic response technique. *J. Mater. Res. Technol.* **2020**, *9*, 4450–4458. [CrossRef]
92. Chopra, A.K.; Goel, R.K. Building period formulas for estimating seismic displacements. *Earthq. Spectra* **2000**, *16*, 533–536. [CrossRef]
93. Hong, L.-L.; Hwang, W.-L. Empirical formula for fundamental vibration periods of reinforced concrete buildings in Taiwan. *Earthq. Eng. Struct. Dyn.* **2000**, *29*, 327–337. [CrossRef]
94. Crowley, H.; Pinho, R. Simplified equations for estimating the period of vibration of existing buildings. In Proceedings of the First European Conference on Earthquake Engineering and Seismology, Geneva, Switzerland, 3–8 September 2006; p. 1122.
95. Guler, K.; Yuksel, E.; Kocak, A. Estimation of the fundamental vibration period of existing RC buildings in Turkey utilizing ambient vibration records. *J. Earthq. Eng.* **2008**, *12*, 140–150. [CrossRef]
96. Hatzigeorgiou, G.D.; Kanapitsas, G. Evaluation of fundamental period of low-rise and mid-rise reinforced concrete buildings. *Earthq. Eng. Struct. Dyn.* **2013**, *42*, 1599–1616. [CrossRef]
97. Yiğit, A.; Erdil, B.; Akkaya, I. A simplified fundamental period equation for RC buildings. *Građevinar* **2021**, *73*, 483–497.

98. Raja, A.; Gopikrishnan, T. Drought prediction and validation for desert region using machine learning methods. *Int. J. Adv. Comput. Sci. Appl.* **2022**, *13*, 47–53. [CrossRef]
99. Kasi, V.; Yeditha, P.K.; Rathinasamy, M.; Pinninti, R.; Landa, S.R.; Sangamreddi, C.; Dandu Radha, P.R. A novel method to improve vertical accuracy of CARTOSAT DEM using machine learning models. *Earth Sci. Inform.* **2020**, *13*, 1139–1150. [CrossRef]
100. Bülbül, M.A.; Harirchian, E.; Işık, M.F.; Aghakouchaki Hosseini, S.E.; Işık, E. A hybrid ANN-GA model for an automated rapid vulnerability assessment of existing RC buildings. *Appl. Sci.* **2022**, *12*, 5138. [CrossRef]
101. Harirchian, E.; Aghakouchaki Hosseini, S.E.; Jadhav, K.; Kumari, V.; Rasulzade, S.; Işık, E.; Wasif, M.; Lahmer, T. A review on application of soft computing techniques for the rapid visual safety evaluation and damage classification of existing buildings. *J. Build. Eng.* **2021**, *43*, 102536. [CrossRef]
102. Bülbül, M.A.; Öztürk, C. Optimization, modeling and implementation of plant water consumption control using genetic algorithm and artificial neural network in a hybrid structure. *Arab. J. Sci. Eng.* **2022**, *47*, 2329–2343. [CrossRef]
103. Bülbül, M.A.; Öztürk, C.; Işık, M.F. Optimization of climatic conditions affecting determination of the amount of water needed by plants in relation to their life cycle with particle swarm optimization, and determining the optimum irrigation schedule. *Comput. J.* **2022**, *65*, 2654–2663. [CrossRef]
104. *TERMFHB-2017*; Tarihi Yapılar için Deprem Risklerinin Yönetimi Kılavuzu (TYDRYK). Vakıflar Genel Müdürlüğü: Ankara, Türkiye, 2017.

Disclaimer/Publisher's Note: The statements, opinions and data contained in all publications are solely those of the individual author(s) and contributor(s) and not of MDPI and/or the editor(s). MDPI and/or the editor(s) disclaim responsibility for any injury to people or property resulting from any ideas, methods, instructions or products referred to in the content.